NUREG/CR--5426

TI89 016813

Examination of the Use of Continuum Versus Discontinuum Models for Design and Performance Assessment for the Yucca Mountain Site

Manuscript Completed: July 1989
Date Published: August 1989

Prepared by
M. Board

Itasca Consulting Group, Inc.
1313 5th Street SE, Suite 210
Minneapolis, MN 55414

Prepared for
Division of High-Level Waste Management
Office of Nuclear Material Safety and Safeguards
U.S. Nuclear Regulatory Commission
Washington, DC 20555
NRC FIN D1016

DISCLAIMER

ABSTRACT

This report examines the use of continuum and discontinuum numerical methods for analysis of the thermomechanical response of the rock mass at Yucca Mountain. Continuum numerical methods consider the rock to be a solid, unfractured body, whereas the discontinuum method is formulated specifically to account for the effects of discrete fractures. The fractures within the rock introduce overall non-linear material response due to slip and separation of rock blocks. Continuum models attempt to simulate this response through the use of non-linear constitutive laws. Discontinuum methods attempt to simulate the true response of the rock mass by correctly modeling the behavior of the joints as well as the deformability of the intact rock blocks. It is shown that, as the joint spacing, s, becomes small with respect to the size of the excavations, the behavior of the jointed rock approaches that of a solid with a form of elasto-plastic constitutive behavior.

It is concluded that a continuum model with a form of "ubiquitous" or "compliant joint" plasticity law is probably sufficient for analysis of the thermomechanical response of excavations in welded tuff. However, one of the questions concerning Yucca Mountain which remains is the effect of fault structures on the stability and performance of the repository, particularly under thermal and dynamic loads. Here, a true discontinuum approach seems necessary.

TABLE OF CONTENTS

TABLE OF CONTENTS
(continued)

LIST OF FIGURES

LIST OF FIGURES
(continued)

LIST OF FIGURES
(continued)

LIST OF FIGURES
(continued)

LIST OF TABLES

1.0 SUMMARY

The disposal of high-level radioactive waste at the Yucca Mountain site in Nevada is proposed for the unsaturated Topopah Springs formation [U.S. DOE, 1988(b)]. The Topopah Springs is a heavily fractured, welded tuff. The proposed repository location lies above the water table within a region cut by several known fault structures. The disposal area is bounded by fault structures on several sides and is cut by the Ghost Dance fault which runs roughly through the center of the emplacement area.

The design of the repository emplacement rooms and layout, the waste emplacement scheme and the thermal, mechanical and hydrochemical performance of the rock mass will be accomplished through the use of models. "Models", here, refers not strictly to numerical models, but to any calculational procedure which attempts to represent the response of the rock mass through some mathematical or empirical formulation. Thus, a model may be analytical, numerical or empirical in nature. Empirical models tend to be used heavily in standard mine design, but are of limited use here since there is no precedent for thermomechanical loading of rock masses, excavations, and their supports at the geometric scale considered. Therefore, to assess performance, and to accomplish the underground design to a great extent, mathematical models are required.

The tuffs comprising the Yucca Mountain site are heavily fractured on a small scale (i.e., meters) due to natural jointing of the rock, but they are also cut by numerous fault planes which can be continuous over thousands of meters. These two general classifications of fracturing (closely-spaced "ubiquitous" jointing and discrete faulting) may impact the repository design and performance in different ways. The tuff jointing may impact emplacement drift or borehole stability, as well as the movement of fluid through the rock mass. The presence of continuous fault structures may have a localized, but more severe, influence on opening stability. Problems such as wedge failure at fault-drift intersections may result from gravitational, thermal or seismic stresses. Fluid migration along fault planes may represent more closely flow in a conduit rather than percolation through a uniformly-fractured continuum.

This report reviews the use of continuum (jointing or fracturing represented via an equivalent continuum material law versus discontinuum (joints and fractures modeled as discrete interfaces which may close, slip or separate) representations of the tuff in numerical modeling at Yucca Mountain. Only the mechanical aspects of continuum and discontinuum representations are discussed here.

It is shown that the type of modeling approach is largely dependent on the geometric scale of the problem to be analyzed. It is concluded that the closely-spaced jointing in the Topopah Springs formation is probably well suited to a continuum joint representation; however, the predominant vertical orientation of the joints probably requires a model which can account for anisotropy in the rock mass response. The faults may have an influence on rock stability around emplacement drifts and boreholes. Slip on faults or wedge failures could have some potential impacts on retrieval operations or the functioning of seals. The response of faults to gravitational, thermal and seismic stress changes can be assessed realistically only by models which can examine the response of discrete planes of weakness. This includes continuum models which incorporate frictional, slipping interfaces or a true discontinuum method.

2.0 APPROACH TO MODELING IN ROCK

2.1 Introduction

The use of models to simulate the mechanical behavior of rock is based on a knowledge of stress-strain behavior of the rock, which varies depending on the scale of the sample which is stressed. Figure 1 illustrates the progression in scale from blocks of intact rock to large volumes of the rock mass. The intact rock material may behave as an elastic solid under the applied stress state, with continued departure from linearity as the "sample" size increases. This is particularly true near the excavation, where confining stresses are low and non-linear response controlled by slip on joint surfaces may dominate. The type of mechanical model which may apply at any scale will depend on factors such as the size of the opening, the joint spacing, orientation and strength of the discontinuities, and the orientation and magnitude of the stress field.

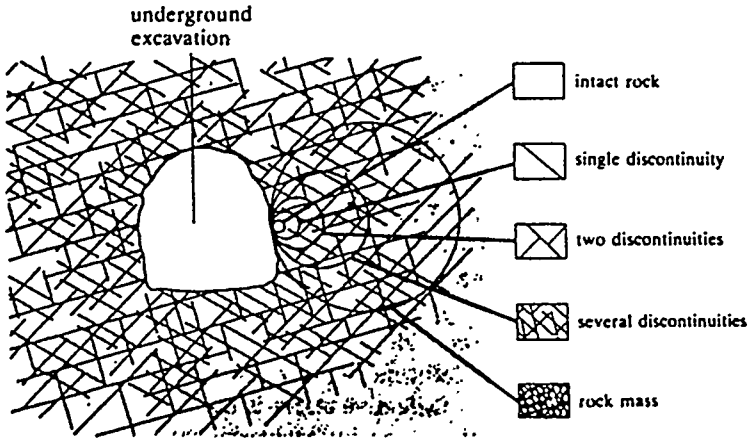

Fig. 1 Illustration of a Jointed Rock Mass Showing the Transition from Intact Rock to Rock Mass As a Function of Geometric Scale [Brady and Brown, 1985]

The phenomena of concern to modeling for nuclear waste disposal are also a direct function of scale. The stability of the emplacement boreholes requires simulation of a volume several meters on a side; the examination of room stability involves volumes of tens of cubic meters; and, the thermal and mechanical effects of the repository involve volumes of hundreds to thousands of cubic meters. In each case, the volume of the excavation in relation to the discontinuity spacing must be examined to determine the appropriate type of model to be used.

There are, in general, two approaches to modeling in rock. In the first approach, the rock mass may be considered to be a discontinuum composed of individual blocks which interact with their neighbors via stiffness and plasticity, introduced by the intervening fractures. The second approach is to model the rock mass as a continuum in which non-linearities (if any) are accounted for through the material model chosen. In practical terms, the former approach allows yield to occur anisotropically or along specific structures within the rock mass (e.g., sliding of a wedge into an opening). The latter approach may allow complex non-linear material models but might not adequately represent discontinuum response such as slip and separation of blocks of material. In particular, wedges or blocks of material may be kinematically constrained with a continuum model due to the inability of the material to separate or slip along discrete weakness planes. The type of approach to be used is a function of the scale of the problem (i.e., relation of spacing of discontinuities to excavation size), the intact rock and joint properties, and the applied stresses.

Figure 2 illustrates the problem of scale and suitable model type through a series of simple examples. The mechanical effects of a borehole in a hard rock with widely-spaced joints may be analyzed by ignoring the presence of the joints and assuming the rock is an elastic continuum. The stability of a room in rock with a joint spacing of roughly 1/4 to 1/5 of the span may be characterized by wedge failure. In this case, the failure mechanism is kinematically controlled by individual discontinuities and not particularly amenable to a continuum representation. If, however, the rock mass is heavily fractured (the discontinuity spacing much smaller than the span), it will act roughly as a granular medium and can be represented by a continuum model. A scheme is presented later which addresses the appropriate model based on the relationship of stress state, excavation dimensions, and joint spacing.

PURPOSE OF SIMULATION	PROBABLE SUITABLE MODEL TYPE
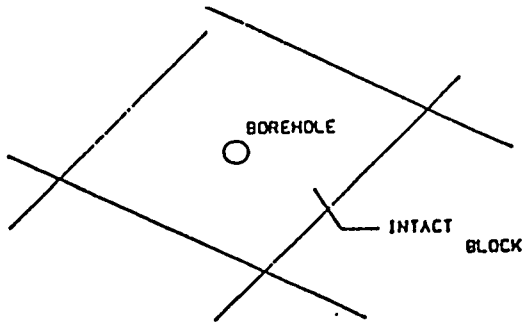 (a) to determine stress induced by hole excavation	continuum, elastic, analytic calculation
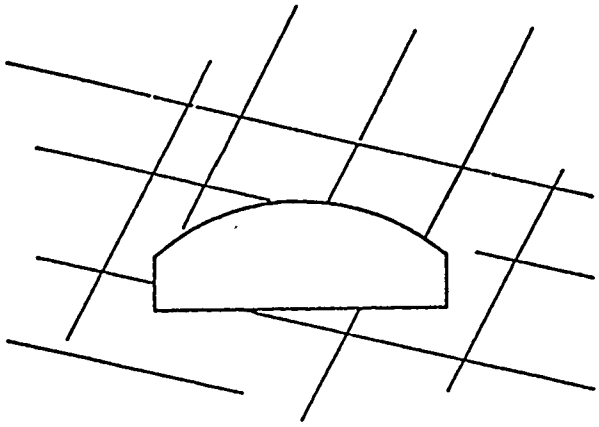 (b) to determine stability of room roof and walls to sliding and gravity fallout	discontinuum or possible analytical calculation
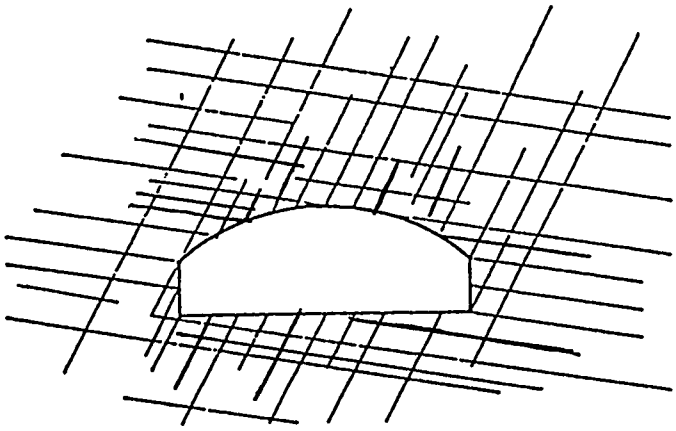 (c) to determine general stability of opening	continuum model with non-linear constitutive law

Fig. 2 Illustration of Relationship of Joint Spacing and Excavation Span to Model Methodology for Hard Rock

2.2 Model Types

2.2.1 Discontinuum Modeling

2.2.1.1 Basis of the Method

The initial development of discontinuum analysis was conducted by Trollope (Stagg and Zienkiewiz, 1968), followed by a numerical modeling approach by Cundall (1971). The early models consisted of rigid blocks with intervening joint surfaces governed by the Mohr-Coulomb yield criterion. Further refinements in the method have led to the Universal Distinct Element Code (UDEC) [Itasca, 1989] in two dimensions and the three-dimensional distinct element codes 3DEC (Itasca, 1988(a), Lemos, 1987), and CICE (Hocking et al., 1985). Some of these codes incorporate automated statistical generation of joints, various joint constitutive laws, internal discretization of blocks (i.e., deformability), dynamics, etc. In addition to the distinct element method, some continuum codes may include interfaces or joint elements upon which slip (and, in some codes, separation) may occur (e.g., Itasca, 1988(b); Biffle, 1984; Stone et al., 1985). These approaches are usually limited to a small number of interfaces which are not allowed to intersect. Therefore, interfaces in continuum codes are restricted, in practical applications, to modeling of a small number of discrete features such as faults or bedding planes. A brief description of the distinct element method follows.

The distinct element method is based on the notion that a rock mass is composed of a series of blocks which interact across the intervening joint planes. The stiffness, friction, dilation, and cohesion properties of these planes may be represented by constitutive laws of varying complexity—the simplest model being the standard Mohr-Coulomb model. This is represented in Fig. 3 as the spring-slider system which governs force transmission at block contact points. The simplest incremental force-displacement law assumes a linear relation for normal and shear components (Fig. 4):

$$\Delta F_n = k_n \, \Delta u_n$$
$$\Delta F_s = k_s \, \Delta u_s \qquad (1)$$

where k_n, k_s = normal and shear stiffness, respectively, and

Δu_n, Δu_s = incremental displacements.

The maximum shear force is limited by the yield function:

$$|F_s| \leq cA + F_n \tan(\phi+i) \qquad (2)$$

where c = cohesion,

A = joint area, and

ϕ,i = friction and dilation angles, respectively.

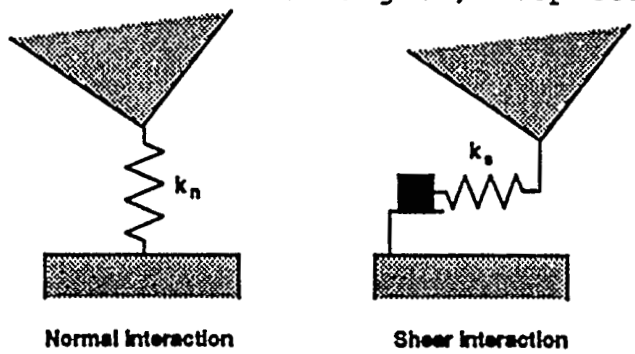

Fig. 3 Interaction Between Blocks Is Governed by the Normal and Shear Stiffness of Their Contacts As Illustrated by the Normal and Shear Springs

NORMAL FORCE:

$F_n = K_n U_n$

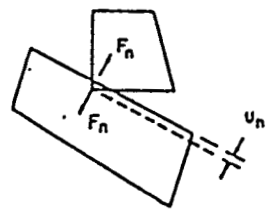

FORCES RESOLVED INTO X and Y DIRECTION AND SUMMED INTO THREE RESULTANTS:

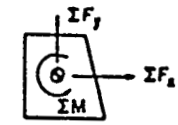

MOTION LAWS:

$$\dot{u}_i = \dot{u}_i + \left(\frac{\Sigma F_i}{m} + g_i\right)\Delta t \qquad \dot{\theta} = \dot{\theta} + \frac{\Sigma M}{I}\Delta t$$

$$u_i = u_i + \dot{u}_i \Delta t \qquad \theta = \theta + \dot{\theta}\Delta t$$

SHEAR FORCE:

$\Delta F_s = K_s \Delta U_s$

$|F_s| \leq F_n \tan\phi$ (Friction Law)

If no cohesion or dilation

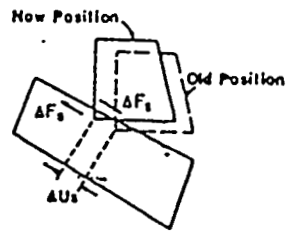

Fig. 4 Simplified Force-Displacement Relations and Motion Equations Used in the Distinct Element Method for Motion of Rigid Blocks

Once the forces applied to the blocks have been determined, the law of motion is used to determine the block accelerations and, thus, their translations and rotations. Internal block deformations may be calculated for any constitutive behavior using internal discretization. From these values, the resultant forces can again be determined by Eqs. (1) and (2). This process is illustrated in Fig. 5 and is repeated until the body is at an equilibrium state or until such time as the system undergoes unstable deformation.

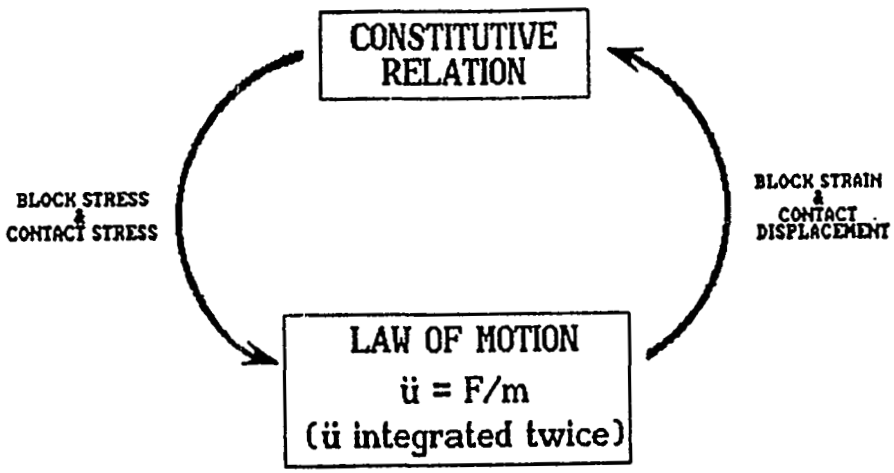

Fig. 5 Calculation Cycle for Explicit Distinct Element Code UDEC

The advantage of this method is that the non-linearities and possible fracture-controlled failure modes of the rock mass may be modeled explicitly, provided the geometry and properties of the joints are known. The problem lies in the determination of the level of detail necessary in the discretization of the rock mass to model the dominant mechanisms. It is not reasonable to attempt to model, over a large area, the complete rock structure of a heavily-jointed rock mass with distinct elements. Reasonable run times, even on high-speed mainframe computers, may limit the problem size to several thousand blocks. Problems such as the stability of single excavations and boreholes, or of fault planes intersecting the repository horizon, may be modeled efficiently with this method.

2.2.1.2 Models of Joint Behavior Used in Discontinuum Models

Two approaches have been followed in formulation of descriptive models of joint behavior. In the first, results from laboratory tests, field observations or conceptual studies have been applied in the proposal of expressions reflecting the dominant aspects of joint behavior. Arbitrary constants appearing in the expressions are then derived from experiment or observation, reconciling response predicted from the model with observed performance. Empirical models derived in this way may not satisfy the laws of deformable body mechanics, but they have the engineering utility of providing techniques for immediate practical solution of current engineering problems.

An alternative to the empirical approach is the formal analytical development of constitutive equations for a joint, ensuring the equations of continuum mechanics are properly satisfied. This approach may seek to derive the constitutive relations from consideration of the morphology of a joint surface and the micromechanics of surface deformation. Input experimental data to such a model are the description of the joint geometry and the mechanical properties of the rock material.

Because of the state of development of several empirical models of joint behavior, it is useful to consider the formulation of each model, and how well behaved each is, under the conditions of non-monotonic normal and shear loading characteristic of a load path experienced by a joint in situ.

(a) Mohr-Coulomb Model — In this simple model (described previously), the joint behavior is described by linear shear and normal stiffness and constant friction and dilation angles. Because the joint surface is rough and non-planar, the normal stiffness will be non-linear and the asperities will shear off during shear deformation. This results in a peak shear strength followed by softening to some residual level. The Mohr-Coulomb model has been criticized for its lack of ability of model these phenomena.

(b) Barton-Bandis Model — Starting from an expression proposed in the early 1970s, for shear strength of a joint, Barton et al. (1985) proposed a comprehensive empirical model for joint deformation mechanics. For purposes of comparison with other joint models, the following summary is presented.

Closure Under Normal Stress:

$$\sigma_n = \Delta V_j / (a - b\Delta V_j) \qquad (3)$$

where σ_n is the normal stress,

ΔV_j is joint closure,

a and b are experimentally-determined parameters,

$a = 1/K_{ni}$, and

K_{ni} is the initial stiffness.

Behavior Under Shear Displacement: Barton's original expression for shear strength of a joint was given by

$$\tau = c + \sigma_n \tan \left(JRC \log \left[\frac{JCS}{\sigma_n} \right] + \phi_r \right) \qquad (4)$$

where JRC is the joint roughness coefficient,

JCS is the joint-wall compressive strength, and

ϕ_r is the residual angle of friction for the joint.

For shear displacement less than that corresponding to peak strength, it was proposed that the mobilized angle of friction could be related directly to the mobilized roughness:

$$\phi_{mob} = JRC_{mob} \log (JCS/\sigma_n) + \phi_r \qquad (3)$$

Noting that over the range of the shear stress-shear displacement curve, the plots of JRC_{mob}/JRC_{peak} and δ/δ_{peak} are similar for different joints, Barton et al. (1985) proposed that a standard look-up table could be employed to interpolate JRC_{mob}/JRC_{peak} from δ/δ_{peak}. Shear displacement δ_{peak} corresponding to peak shear resistance was proposed to be related to specimen dimensions by the expression

$$\delta_{peak} = \frac{L_n}{500} \left[\frac{JRC_n}{L_n} \right]^{0.33} \quad (6)$$

where subscript n relates to the field scale shear unit, and L defines the length of the shear unit.

Size Effects: One of the more controversial aspects of the Barton-Bandis model is the postulated existence of size or scale effects (to be distinguished from the surface roughness effects considered previously). A series of shear tests on model joints, in which some joints were sectioned and tested to assess notional effects of scale, suggested both JCS and JRC were related to the size of the shear surface. For subscripts o, indicating laboratory scale, and n, denoting field scale, the scaling relations between laboratory and field values of JRC and JCS are proposed to be

$$JRC_n = JRC_o \left[\frac{L_n}{L_o} \right]^{-0.02JRC_o}$$

$$JCS_n = JCS_o \left[\frac{L_n}{L_o} \right]^{0.03JRC_o} \quad (7)$$

Equations (3)-(7) indicate that from measured values of a, b, JCS, JRC and ϕ_r (which can be obtained in simple tests), it is possible to predict the deformation of a joint through any imposed stress or displacement path (Some extensions of the model provide information on joint hydraulic properties under load as well). The model is widely applied in predicting the hydromechanical behavior of rock masses. In spite of its widespread application, some difficulties with the model need to be recorded.

The first problem involves the arbitrary nature of some of the parameter definitions. For example, Eq. (4) is usually cast as

$$\tau = c + \sigma_n \tan (i + \phi) \quad (8)$$

where i is the effective roughness angle for the surface.

Since $i = JRC \log(JCS/\sigma_n)$, it is implied that $i = JRC$ when $\sigma_n = 0.1JCS$. It is improbable that such an arbitrary definition of i could adequately predict the dilation angle for joints under low normal stress, as is required by established use of the roughness angle concept.

A second difficulty arises when $\sigma_n > JCS$. In this case, i becomes negative, yielding an effective friction angle $(\phi_r + i)$ less than the residual friction angle, which is logically impossible. This suggests that Eq. (3), proposed from joint shear tests at relatively low normal stress, is not appropriate to the stress levels generated in subsurface engineering practice.

An interesting feature of the model is that it assumes no reduction in roughness over a significant proportion of the prepeak range of shear displacement. This implies a joint cycled in shear in this range would achieve a peak strength unaffected by cycling, when the load was subsequently monotonically increased. This is in direct contrast to the experimental observations of Brown and Hudson (1974).

A final point of concern about the model is the pronounced significance of scale effects. Equations 7 were derived from model tests in which joint specimens were sectioned, to determine the effect of the same joint surface tested at different length scales. The description of the experiment, indicated by Fig. 6, suggests that specimen height/width ratio varied in the test. It is possible that the associated change in loading conditions for the shear surface, arising from specimen constraint and geometry, has contributed to the purported size effects.

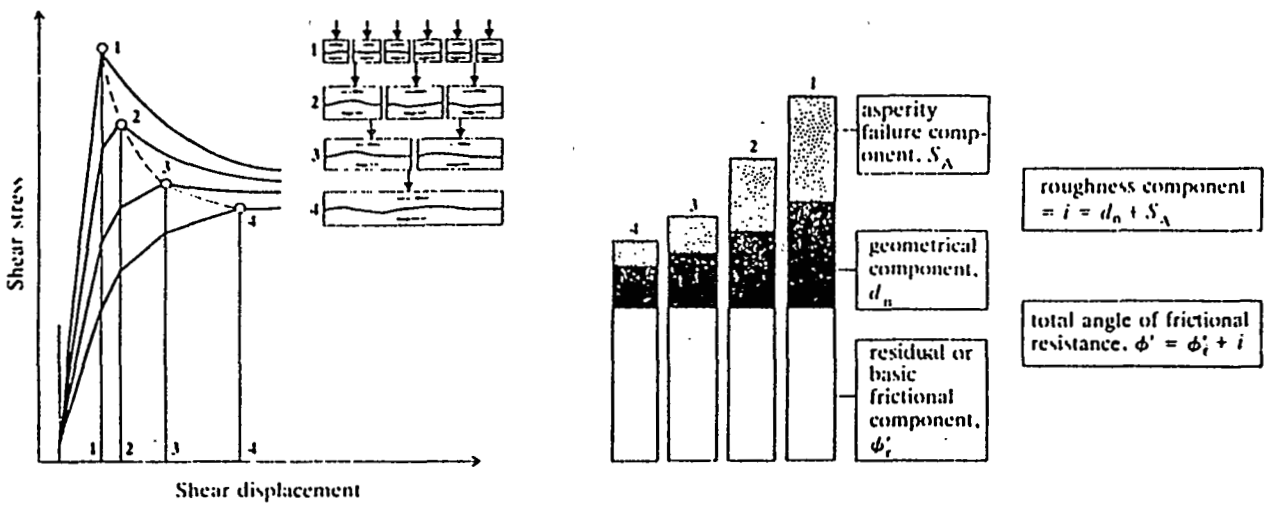

Fig. 6 Experimental Determination of Scale Effects for Joint Shear Strength [Barton et al., 1985]

(c) Cundall-Lemos Model — This is an empirical joint model, described by Lemos (1987), intended to resolve some of the inconsistencies noted in the Barton-Bandis scheme. It is a damage accumulation model of joint shear, based on the principle that all joint shear displacement results in the progressive erosion of asperities and reduction in dilatancy. In a manner similar to that followed by Barton and Bandis, the model is developed from experimental observations of joint performance under load. Instead of an expression for peak shear strength, however, the initial attention is with the stress-displacement relations for the joint. These are illustrated in Fig. 7.

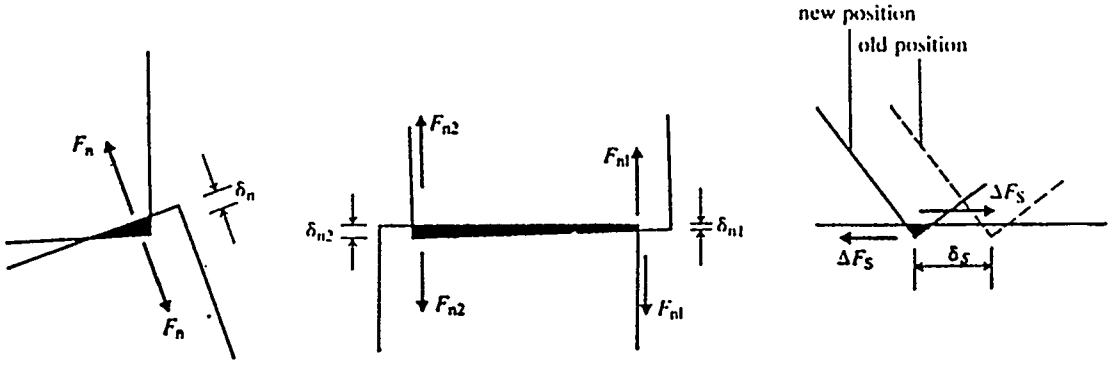

Fig. 7 Normal and Shear Modes of Interaction of Jointed Rock Units [Brady and Brown, 1985]

Joint normal deformation in the model is related to normal stress through the relation

$$\Delta\sigma_n = k_n \, \Delta u_n \tag{9}$$

where k_n, the joint normal stiffness, is normal stress dependent, and is given by

$$k_n = a_n \sigma_n^{\,e_n} \tag{10}$$

where a_n, e_n are model parameters.

In a similar way, the shear stress increment is given by:

$$\Delta\sigma_s = Fk_s \, \Delta u_s \tag{11}$$

where F is a factor which governs the instantaneous slope of the shear stress-displacement curve. The shear stiffness may be related to normal stress in a manner similar to (10); where

$$k_s = a_s \sigma_n^{e_s} \tag{12}$$

In Eq. (11), F is a term representing the fraction of the increment of shear displacement which is elastic and recoverable (the remainder, Δu_s^p being assumed to involve plastic deformation of asperities and to be irrecoverable.) The value of F is obtained from the difference between the prevailing joint shear stress and the ultimate shear strength at the prevailing normal stress, as shown in Fig. 8:

$$F = (1 - \sigma_s/\tau_m)/(1-r) \tag{13}$$

The parameter r in Eq. (13) is introduced to ensure that F approaches unity on reversal of shear load direction.

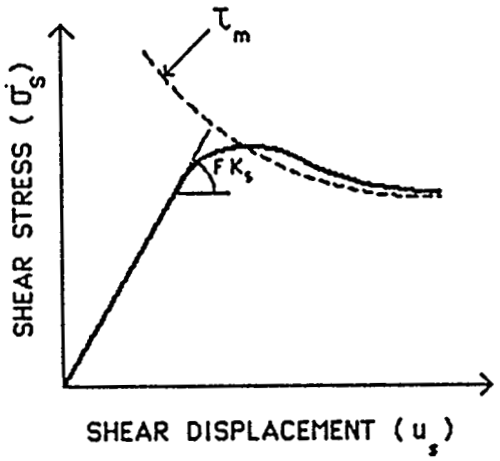

Fig. 8 Shear Stress-Shear Displacement Model and Bounding Shear Strength Curve for Continuously-Yielding Joint Model [Lemos, 1987]

Normal and shear response are coupled in the model through the normal stress dependence of k_n, k_s and F. Also, at any state of normal stress σ_n, shear strength is given by

$$\tau_m = \sigma_n \tan \phi_m \text{ sign } (\Delta u_s) \tag{14}$$

when ϕ_m is the current friction angle.

The friction angle ϕ_m in Eq. (14) takes account of residual friction and a component i related to roughness and dilatancy. The latter component is assumed to be progressively reduced by shear displacement and erosion of asperities, according to

$$\Delta\phi_m = -1/R(\phi_m - \phi_r)\Delta u_s^p \tag{15}$$

where $\Delta u_s^p = (1-F)\Delta u_s$, and

R = a roughness parameter for the surface (having the dimensions of length).

Inspection of Eqs. (9)-(15) indicates that seven parameters are required in this model to characterize a model: a_n, e_n, a_s, e_s, ϕ_m (initial), ϕ_r and R. No conceptual or experimental difficulty is presented for the first six. However, the roughness parameter R is not yet defined in formal detail sufficient to allow its experimental determination.

The Cundall-Lemos model makes no explicit reference to a scale effect. However, it is possible that the length scale defined by the roughness parameter R is sufficient representation of such a phenomenon, if indeed it exists.

Some exercises with the model to demonstrate its performances are shown in Fig. 9. It is seen that, for the particular joint parameters selected,

(1) peak-residual behavior for different initial roughness is modeled satisfactorily [Fig. 9(a)];

(2) a cycle of unloading-reloading shows suitable hysteretic response; and

(3) an episode of pre-peak cyclic loading results in pronounced modification of the shear-stress displacement response, with virtual elimination of peak-residual behavior, consistent with the observations of Brown and Hudson (1974).

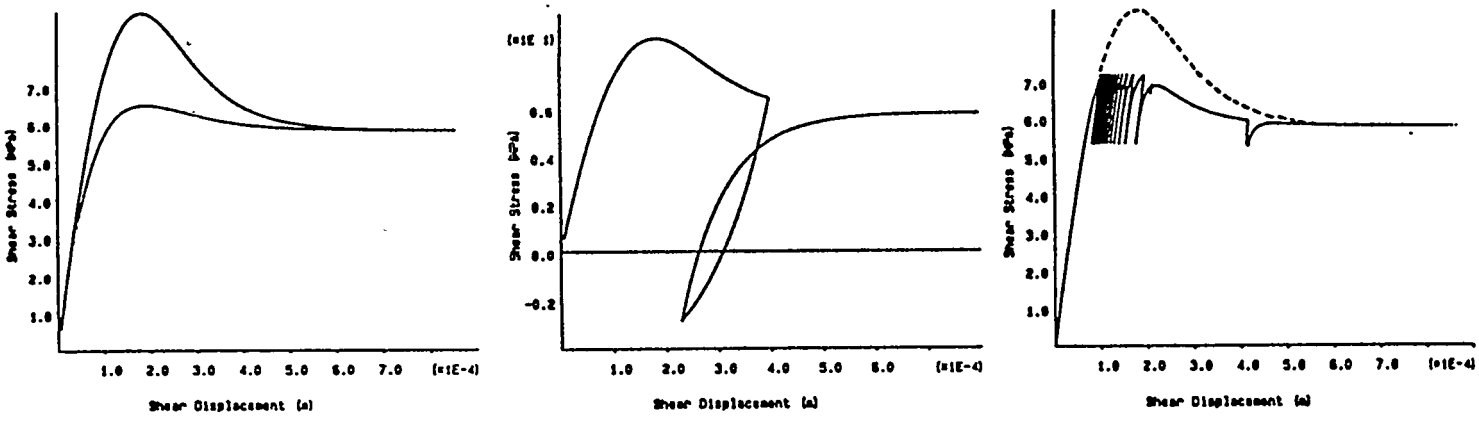

(a) (b) (c)

Fig. 9 Exercising of Cundall-Lemos Model: (a) peak-residual behavior; (b) hysteresis on load reversal; (c) load cycling [Lemos, 1987]

2.2.2 Continuum Models

Continuum models include any numerical technique based on the equations of continuum mechanics in which the assumption is made that holes do not open in a body, or that slip or separation do not occur on discrete weakness planes. Obviously, non-linear behavior of fractured rock is due primarily to slip along existing weakness planes. Continuum models attempt to represent this non-linearity through constitutive laws as described in the sections below. Typical continuum methods include the finite element method (e.g., Zienkiewicz, 1977), the finite difference method (e.g., Cundall, 1976) and the boundary element method (e.g., Banerjee and Butterfield, 1981).

2.2.2.1 Equivalent Elastic and Empirical Models

Equivalent elastic and empirical models are often used for estimates by designers or constructors in the initial stages of a project where little physical property data are available. The principal stresses at varying points around the excavation are calculated using elastic models, and are then input to an empirical failure criterion such as the Hoek-Brown equation:

$$\sigma_1 = \sigma_3 + (m\,\sigma_c\sigma_3 + s\sigma_c^2)^{1/2} \qquad (16)$$

where m,s = empirical curve-fit constants, and

σ_c = uniaxial compressive strength of intact rock.

A "factor of safety" can be determined as the ratio of the calculated-to-failure stress as given by Eq. (16).

This approach appears to be adequate for initial design studies; however, there are some problems associated with its use. The values of m and s are related to the properties of the in-situ rock mass and are not readily available. Hoek and Brown (1988) have presented a subjective list of values for these constants as a function of rock mass type and quality. The suggested values are purportedly conservative, but few field cases have been published in which this design technique has been compared to observation and field instrumentation. It must also be kept in mind that the use of this model is presently considered useful for an estimation of conservatism in design—but not a rigorous method of determining rock mass performance.

A second commonly-used method is to assume that the rock mass behaves as an equivalent elastic continuum (Fig. 10). Here, the presence of jointing or defects in the rock mass are assumed to result in a reduction of the elastic modulus as well as a reduction in its ultimate compressive strength. Typically, the reduction in elastic properties is determined by assuming the rock mass to be isotropic with joints at some spacing, s, with normal and shear stiffnesses, k_n and k_s, respectively. The equivalent elastic modulus may be determined by assuming that the jointed and equivalent mass undergo an equal displacement for equal applied stress, σ (see, for example, Singh, 1973; Goodman, 1981). The following relations may be derived:

$$\frac{1}{E_i} + \frac{1}{k_n s} = \frac{1}{E_e}$$

$$\frac{1}{G_{xyi}} + \frac{1}{k_s s} = \frac{1}{G_{xye}} \qquad (17)$$

where E_i = intact Young's modulus,

E_e = equivalent Young's modulus,

G_{xyi} = intact shear modulus, and

G_{xye} = equivalent shear modulus.

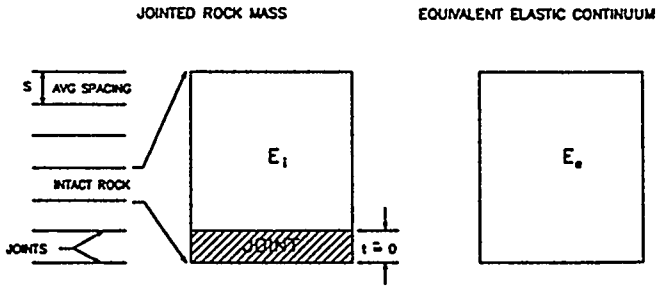

Fig. 10 Equivalent Elastic Continuum Determined by Treating the Model as a Series of Intact Blocks Connected with Joints Treated as Shear and Normal Springs (One-, two- and three-dimensional regular and random jointed equivalent models have been developed.)

A plot of the ratio of the elastic modulus to equivalent modulus as a function of normal stiffness and joint spacing is given in Fig. 11. Fossum (1985) and Gerrard [1982(a); 1982(b)] have given models for equivalent elastic continua for randomly and regularly jointed masses in two and three dimensions. Others have suggested relationships for empirical rock mass classifications and the elastic modulus. Bieniawski (1978) suggested that, for rocks with a rock mass rating (RMR) of 55 or greater, the deformation modulus could be approximated by

$$E_e = 2(RMR) - 100 \qquad (18)$$

where E_e = equivalent modulus (GPa), and

RMR = rock mass rating.

Again, there is little field data which support these relations.

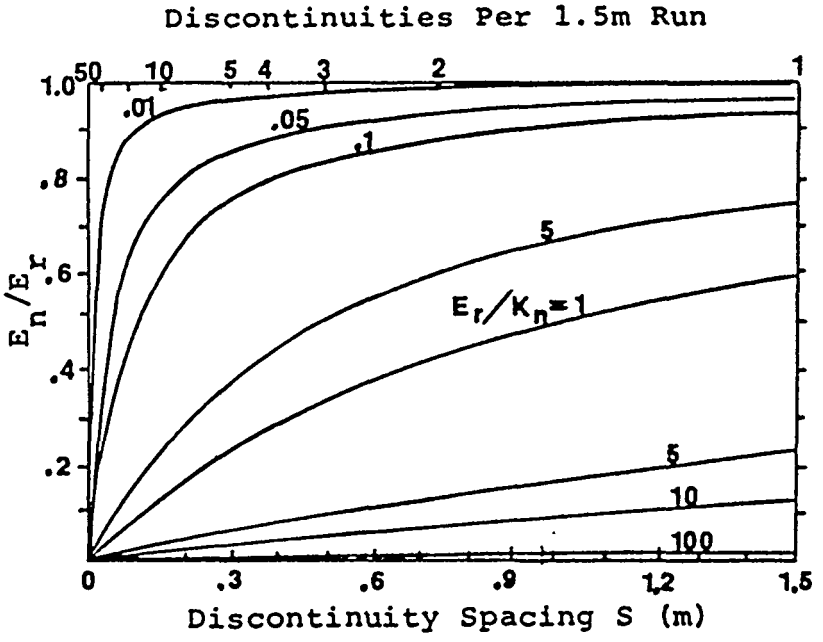

Fig. 11 Ratio of Rock Mass Modulus (E_n) to Intact Modulus (E_r) As a Function of Discontinuity Spacing and Joint Normal Stiffness [Kulhawy, 1978]

In general practice, equivalent moduli are often determined from field compression experiments such as block tests, borehole jacking tests, flatjack tests, or plate-bearing tests. This method may work well in instances where the rock mass response is truly elastic in the working stress range, but it can lead to significant errors in instances where the behavior is non-elastic.

Blanford and Key (1987) used an equivalent elastic continuum model within the SANCHO code (Stone et al., 1985) to compare to field results of an 0.8m square flatjack slot test. This equi-

valent continuum model is a bit more elaborate in that the normal stiffness of the joints is assumed to be a non-linear function of normal stress. The following hyperbolic representation was developed by Bandis (1980) and is based on laboratory testing of joints.

$$\sigma_n = \frac{-\delta_n}{a - b\delta_n} \tag{19}$$

where σ_n = normal stress,

δ_n = normal closure, and

a,b = constants, reciprocals of the initial normal stiffness and half-closure stress, respectively.

The normal stiffness is the slope of the $\sigma_n - \delta_n$ curve:

$$k_n = \frac{(1 - b\sigma_n)^2}{a} \tag{20}$$

The in-situ modulus can be found as before:

$$\frac{1}{E_e} = \frac{1}{E_i} + \frac{1}{k_n s}$$

or

$$E_e = \left[\frac{1}{E_i} + \frac{a}{s(1 - b\sigma_n)^2} \right]^{-1}$$

The equivalent elastic models are attractive because the computational requirements are not extensive, input properties are reasonably easily obtained from laboratory testing and/or empirical data. The interpretation of the results from an elastic model is also straightforward. As with any model, the equivalent elastic approach must be compared with field data to define the limits of its applicability.

2.2.2.2 Equivalent Non-Linear Models

One of the most common modeling approaches is to assume that the rock mass behaves according to some non-linear constitutive law. The non-linearity in the constitutive law represents the effects of the defects (e.g., fractures) in the rock structure on its overall mechanical response. The various schemes of representing non-linear behavior in rock may be divided into the following two groups (Desai and Christian, 1977):

(1) representation of stress-strain curves by curve-fitting; and

(2) plasticity theories.

Curve-Fitting

Curve-fitting is a common method of describing stress-strain behavior for rock. The Hoek and Brown criteria described previously is one example where a non-linear curve has been fit to existing triaxial test principal stress data using two parameters, m and s. In viscous rocks (e.g., salt), power law functions comprise one of the primary means of describing creep behavior.

Yield can be simulated numerically by adjusting the elastic modulus of the material in a series of linear increments to model non-linear behavior. The simplest form is a bi-linear model (Fig. 12) which simulates hardening or yield by a stiffening or relaxation in the elastic modulus.

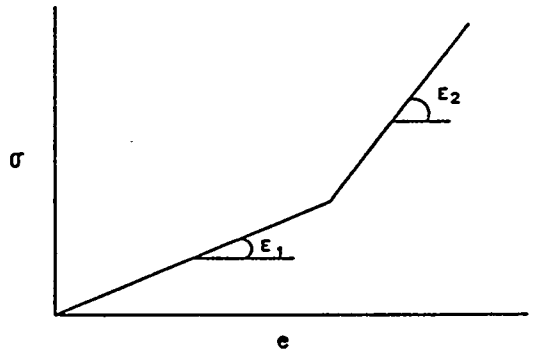

Fig. 12 Simple Bi-Linear Stress-Strain Curve

Greater detail may be obtained by using a greater number of linear segments to define the stress-strain curve. A bi-linear model was used by Hocking et al. (1985) to describe the stress-strain behavior of basalt at the Near Surface Test Facility (NSTF) for the Basalt Waste Isolation Project. An initial low modulus was used to model the closing of joints at low stress levels, followed by a modulus increase as blocks tend to lock up.

There are two primary problems with use of modulus adjustment to describe non-linear stress-strain curves. First, the unloading behavior is not properly modeled because unloading occurs along the loading line and no plastic strains are accumulated. Second, the curve-fitting model does not reproduce the proper flow rule upon yield, resulting in incorrect calculation of strain rate magnitude and direction after yield. The degree of error depends on the extent of yield in the model. An important point is that curve-fitting schemes do not attempt to model the actual deformation mechanisms; therefore, there is often little theoretical basis for them.

Plasticity Models

There are several forms of plasticity which are used to represent rock behavior. Typical models include (Fig. 13): (1) rigid, perfectly-plastic; (2) elastic, perfectly-plastic; and (3) some form of work hardening or softening. In each case, a yield criterion or function is used to describe the stress conditions under which failure of the material occurs. The two simplest yield functions (the Tresca and the von Mises) assume that the material is non-frictional and are more appropriate for metals. The two most common yield criteria for rock are the Mohr-Coulomb and the Drucker-Prager criteria. Here, the material is treated as frictional and cohesive. Figure 14 illustrates the Mohr-Coulomb criterion given by:

$$\sigma_1 - \sigma_3 = (\sigma_1 + \sigma_3)\sin\phi + 2c(\cos\phi) \qquad (21)$$

where σ_1, σ_3 = maximum, minimum principal stresses,

ϕ = friction angle, and

c = cohesion.

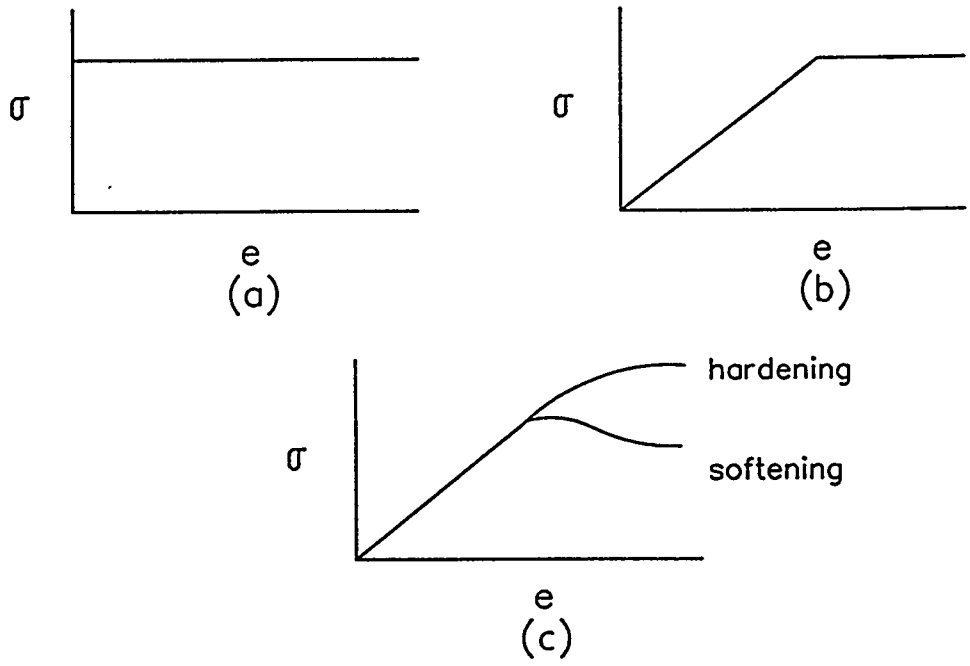

Fig. 13 Three Plasticity Models Typically Used to Represent Rock: (a) rigid-perfectly plastic; (b) elastic-perfectly plastic; and (c) strain-hardening/softening

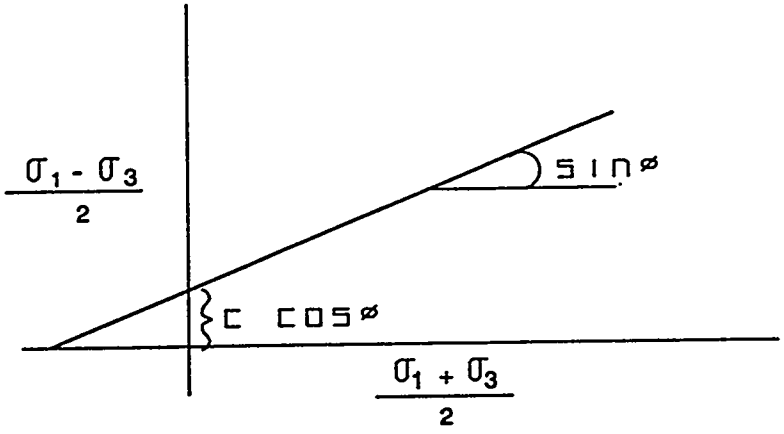

Fig. 14 Mohr-Coulomb Yield Criteria

The Drucker-Prager criterion is similar to the Mohr-Coulomb but includes an additional dependency on the intermediate principal stress:

$$(J_2)^{1/2} = k - \alpha I_1 \qquad (22)$$

where $J_2 = \frac{1}{6}[(\sigma_2 - \sigma_3)^2 + (\sigma_3 - \sigma_1)^2 + (\sigma_1 - \sigma_2)^2]$,

$I_1 = \sigma_1 + \sigma_2 + \sigma_3$, and

K, α = constants, functions of ϕ, c.

The above yield criteria determine the limit condition; however, the strain (and displacement) of the body after yielding must consider some rule for relation of stress to strain increment. This relation is termed the "flow rule". An "associated" flow rule, or "normality", are the terms given to describe colinear stress and strain tensors. This is usually as shown it in Fig. 15, where the strain rate increments are aligned to the outward normals of the yield criterion. The normality assumption requires that $\phi=\psi$ (where ψ is the dilation angle). Experimental testing in rock has shown that associated flow overpredicts dilational strains. As a result, "non-associated" flow rules are often used in rock mechanics. Here, the dilation can be defined separately from the friction.

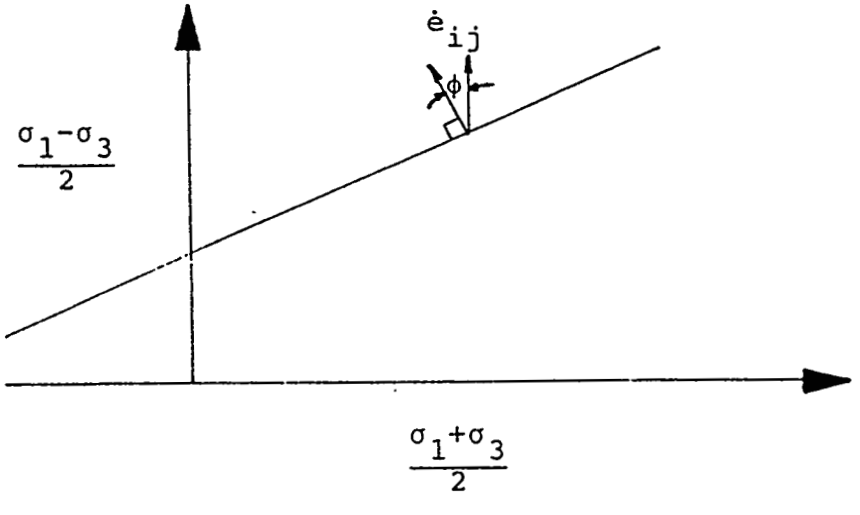

Fig. 15 Strain Rate Increment Tensor For an Associated Flow Rule (It is colinear with the stress tensor; the dilation angle, Ψ, must equal the friction angle, ϕ.)

The standard plasticity formulations described here are isotropic —i.e., the yield response of a body will be the same in all directions, assuming uniform stress conditions. These models are therefore best-suited to conditions where the material is intensely jointed (i.e., where joint spacing is small in comparison to the excavation diameter and where several joint sets exist). In many cases, one, two or three regular sets of joints exist which may result in anisotropic yielding. If the joint spacing is significantly less than the opening dimension, a "ubiquitous" joint, or "compliant" joint, continuum plasticity model may be suitable for use.

Ubiquitous joint models assume, as implied by the name, that one or more joint sets are very closely-spaced and exist everywhere in the rock mass. For an infinite number of these joint planes at all directions within the mass, this model reverts to an isotropic plasticity model. The usual ubiquitous joint model is implemented by first determining the stress state perpendicular and parallel to the structure. This stress state can be compared to the slip condition for the joint—if slip occurs, stresses are adjusted accordingly to keep the stress state for that element on the yield surface. A common limitation exists for the ubiquitous joint models: usually, the material behaves as the matrix in compression and the joint in shear. There is, therefore, no "load sharing" between the matrix and the joint, as stiffness is not assigned to the joints. For this reason, ubiquitous joint models are best applied where fracture frequency is high. Examples of these models can be found in Zienkiewicz and Pande (1977) and Itasca [1988(b)].

Compliant joint models were developed in an attempt to overcome the above limitation of the ubiquitous joint models while providing the computational efficiency of a continuum approach. In general, compliant joint models explicitly account for the spacing of joints for multiple sets as well as non-linear variations of the shear and normal stiffness of the fractures. Examples of compliant joint models can be found in Chen (1987), Costin and Chen (1988), Moreland (1974), and Blanford and Key (1987). In general, these models assume that the joint sets are parallel, continuous, and regularly-spaced. Additionally, it is assumed that the stress is appropriately uniform over the element and that the tractions over the joints within an element are subsequently the same. Thus, the dilation and slip displacement distributions are continuous across each element. The compliant joint model described by Chen (1987) is currently under consideration by NNWSI for use in repository design and performance anal-

ysis. This model presently assumes two perpendicular, regularly-spaced joint sets (Fig. 16) subject to the assumptions described above. The joint normal and shear displacement behavior are shown in Figs. 17 and 18. The hyperbolic normal stiffness behavior of the joint follows Goodman (1976), and requires constants for the maximum joint closure (u^d_{max}) and the half-closure stress. The shear stress-shear strain behavior is bilinear, with the Mohr-Coulomb slip condition governing yield.

Costin and Chen (1988) describe the use of this model for comparison to the results of the G-Tunnel Heated Block Test [Zimmerman et al., 1986(a)]. In this test, an $8m^3$ block of tuff was freed from the floor of a drift by line drilling. Flatjacks were used to load the block biaxially and uniaxially, and horizontal displacements were monitored by recording differential displacement between 1.5 m-long vertical posts grouted in the block (HSX gauges).

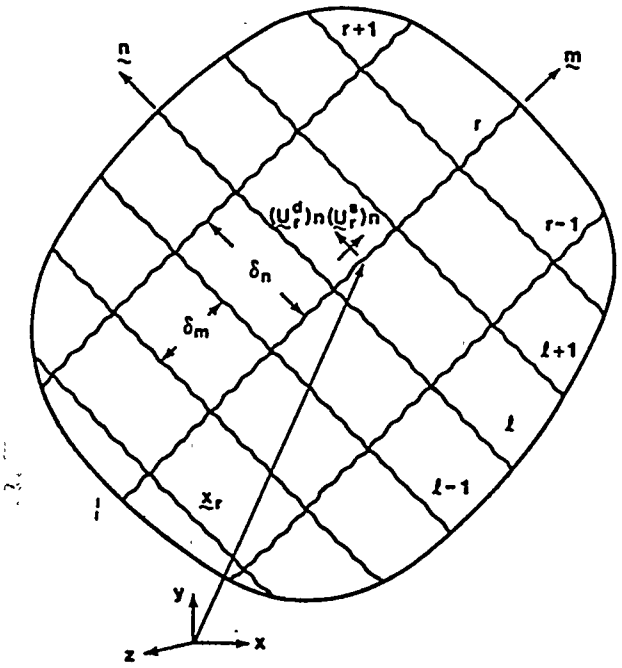

Fig. 16 A Jointed Rock Medium [Chen, 1987]

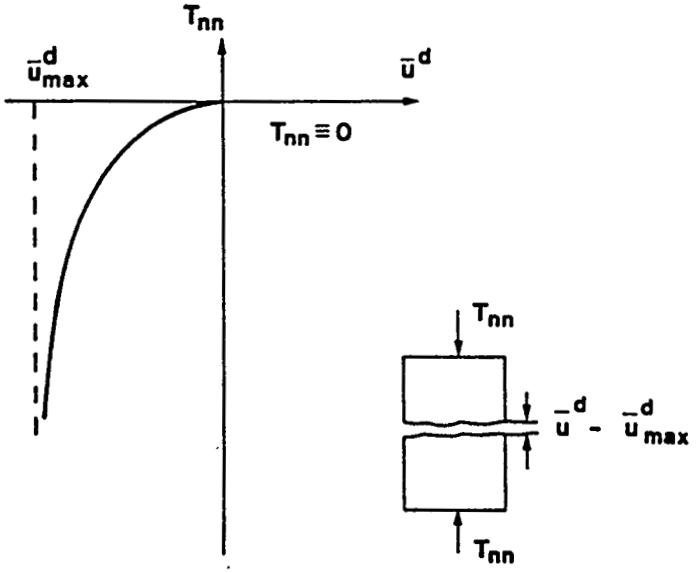

Fig. 17 Non-Linear Elastic Normal Joint Behavior [Chen, 1987]

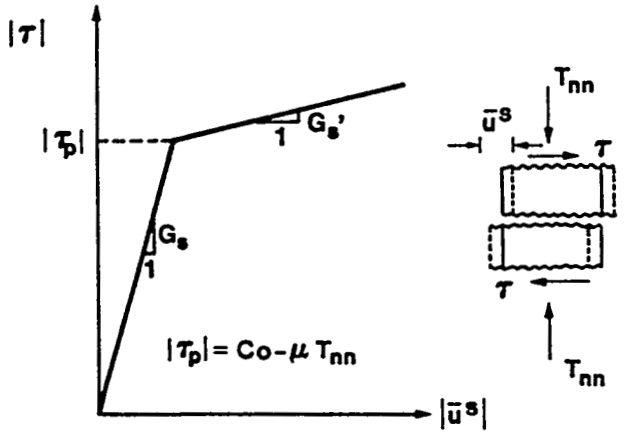

Fig. 18 Non-Linear Shear Behavior of Joints [Chen, 1987]

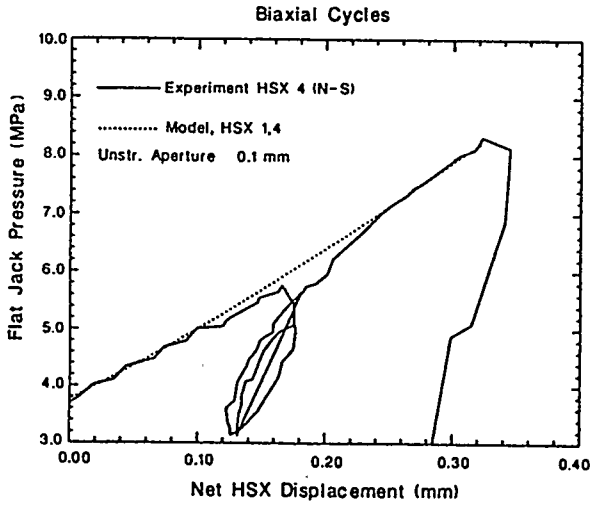

Fig. 19 Comparison Between Calculated and Experimental Data for HSX #4 for Unstressed Aperture of 0.1 mm [Costin and Chen, 1988]

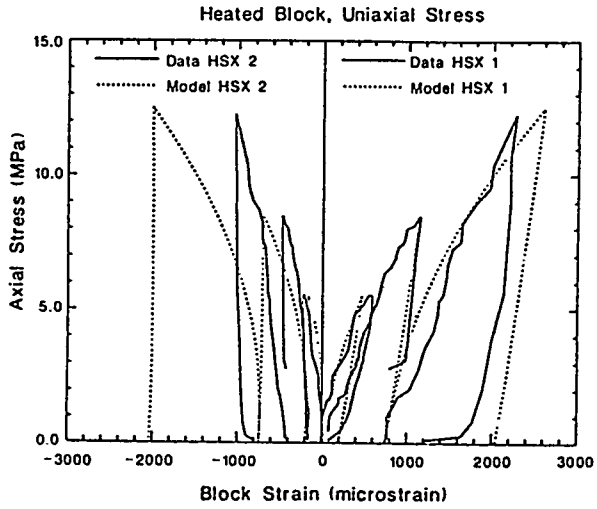

Fig. 20 Comparisons of the Calculated and Experimental Data for Uniaxial Loading Conditions (HSX1 and 2) [Costin and Chen, 1988]

Figures 19 and 20 show comparison of applied stress-horizontal displacement measurements for selected biaxial and uniaxial pressure cycling. The biaxial compression results show that loading behavior can be predicted fairly well with the model. This is not surprising, as the block behaved more-or-less linearly in biaxial compression where slip is minimized. The model does not reproduce the permanent deformations upon unloading. The uniaxial comparisons are fairly good, and illustrate the effects of joint shear displacement on the permanent deformation of the block.

The joint properties which resulted in a best-fit of the data to the model were:

shear stiffness	10^{10} GPa/m
friction coefficient	0.8 (38.6°)
cohesion	0.003 MPa (essentially zero)
unstressed aperture	0.05 mm
half-closure stress	5.0 MPa

Because the applied stress levels were so low, the prediction of response was found to be dependent only on the cohesion.

It is noted that, at the second and third load cycles, the comparison to the response of HSX2 is poor. This may be a result of the inability of a continuum model to adequately represent the kinematic response of a system of blocks. Although not given, it would be quite interesting if additional comparisons had been made in this paper to simple elastic, elastoplastic and ubiquitous joint models. It should also be noted that the applied loading conditions of the block test are simple by design (i.e., uniform biaxial and uniaxial loads). The rock mass surrounding excavations will be subjected to complex loading states in which large stress gradients are applied. The ability of the compliant joint model to determine rock mass failure under high stress gradients is not known at present. Blanford and Key (1987) compare a reduced elastic modulus, compliant joint and quasi-discrete, constitutive models for analysis of the stresses and displacements surrounding a pressurized slot test. It was found that spacing of joints, in combination with applied loading conditions, can have a large effect on the predicted rock mass response from the models. In particular, it was found that a continuum joint response is not appropriate in a case where joint

spacing is of the same order as the excavation, or length across which load is applied. In such a case, the intact blocks perform a significant load-carrying function which a continuum joint model may not be able to adequately model. Here, the quasi-discrete (or distinct element) model is better suited.

2.3 Methodology for Choice of Model Type Under Varying Rock Conditions

Various modeling techniques have been discussed in the previous sections. The question which arises is: Under what circumstances can a rock mass be considered a continuum or a discontinuum? Starfield and Detournay (1981) examined various rock mass conditions typical in design and developed a tentative set of conceptual models for the design of tunnel supports. They identified five (5) typical tunneling conditions:

(1) massive rock (no stress-induced failure, no joint stability problems);

(2) overstress rock conditions (plastic and brittle failure mechanisms);

(3) stress-related failure in low cohesion rocks (shallow and deep conditions);

(4) blocky rock masses; and

(5) swelling rock.

These conditions are illustrated in Fig. 21. A sixth category is added here: isolated fractures which may or may not intersect an excavation. The following descriptions are adapted from Starfield and Detournay (1981).

Model 1 pertains to a tunnel driven in a massive rock mass with few joints. No rock failure is induced, nor is there a joint stability problem. Support, if required, would be in the form of spot reinforcement.

Model 2 pertains to a situation in which excavation of the tunnel leads to rock failure. The rock could either be massive or have a high density of joints. Failure can be brittle (slabbing, rock bumps, bursting) or plastic. If plastic failure is severe, it will lead to squeezing rock conditions.

Model 3 applies to a tunnel driven in a low cohesion rock mass which leads, in severe situations, to running ground conditions.

Model 4 refers to a tunnel with potential structural instability (i.e., instability associated with movements or separation on joints, usually associated with roof problems).

Model 5 characterizes a tunnel in a potential swelling rock (i.e., rock containing anhydrite or a certain amount of sensitive clay materials).

Model 6 applies to a rock with isolated fractures (i.e., a fault) which may or may not intersect excavations.

For each model, the joint spacing, excavation diameter, rock mass stress conditions and rock mass strength parameters are required. Figure 22 provides an algorithm for use of the classification scheme. Three (3) of the models (1, 2 and 4) have the greatest potential for excavation in hard rock. Model 1 pertains to cases where the intact rock is elastic and the spacing of fractures is greater than the excavation span. This is of interest in only a limited number of applications where the rock may be considered an elastic continuum.

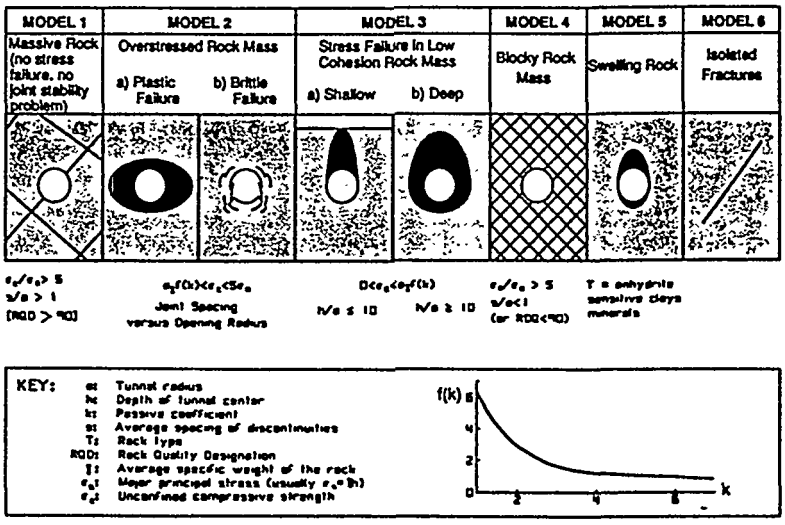

Fig. 21 Models Proposed for Varying Rock Mass Conditions [adapted from Starfield and Detournay, 1981].

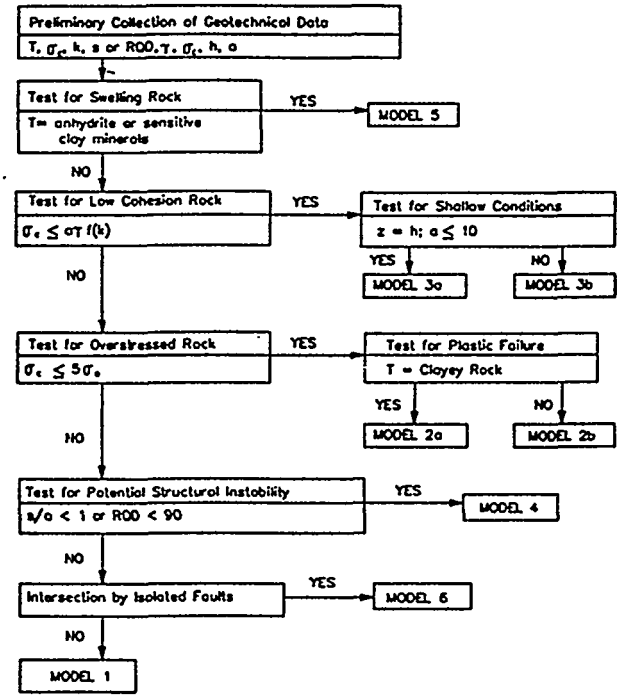

Fig. 22 Model Selection Algorithm

Model 2 pertains to overstressed rock in which failure is evident from plastic or brittle mechanisms. Severe plastic deformation leading to squeezing problems generally occurs in heavily fractured ground with multiple joint sets with ratio of spacing (S) to excavation radius (a) of 0.1 or less. In most cases, high in-situ stress or low friction and cohesion joint surfaces are present. Failure under these conditions may be amenable to isotropic plasticity models or ubiquitous joint models.

Model 4, blocky rock mass classification applies most readily to the expected Topopah Springs excavation conditions. In this classification, instability is concerned with failure mechanisms controlled by the rock mass structure. In the case at Yucca Mountain, it would appear that structural response will be controlled by the predominant vertical joint set, as well as major discontinuities such as faults which may intercept the excavations. It may also be expected that the response will be anisotropic due to the preferred jointing direction.

The response of a blocky rock mass and, thus, the proper choice of model depends on many factors, including:

(1) the number of joint sets;

(2) the spacing of the joints with respect to the radius of the excavation (S/a);

(3) the orientation of the joint sets with one another and with respect to the in-situ stress state;

(4) the magnitude and deviation of the principal stresses;

(5) the friction, cohesion and, to a lesser extent, the dilation of the joint surfaces;

(6) the continuity or length of joints (i.e., are they continuous features over large distance?); and

(7) the planarity of the joints (Items (6) and (7) are sometimes taken together to define,in loose terms, the "degree of interlocking".).

To our knowledge, no study has been published which attempts to quantify the above factors and how they relate the use of continuum and discontinuum models, and the proper choice of constitutive law.

The discontinuum code UDEC (Itasca, 1989) was used to examine plastic yield around tunnels in jointed rock for varying spacings and orientations. The models involve static biaxial loading (σ_V/σ_H = 2/1) of a circular tunnel of radius a in a rock mass with two distinct continuous joint sets with spacing S, oriented at angles $\pm\alpha$ from the vertical. Two basic joint spacings with S/a ratios of 0.333 and 0.083 (3 and 12 joints across the tunnel diameter) were used. The maximum principal stress direction is vertical, and joint sets are oriented at ±45°, -15°/-70° and 65°/-60°. The results presented here compare the yield zone at equilibrium for the varying case studies. Figures 23 and 24 show the cases for joints oriented at ±45° for S/a of 0.333(a) and 0.083(b). The yielded elements, shown by a cross at their centroid, are much the same for these joint spacings.

The effect of joint orientation on yield is shown in Fig. 25 for S/a ratio of 0.167 and joint set angles of -15°/-70° and 65°/-60°. In the first case, the -15° joint set is aligned at a small angle to the maximum principal stress, resulting in a large shearing stress component. In this case, anisotropy in the yield zone occurs following along the direction of favorably oriented structures. In the second case, the two low angle joint sets promote a horizontal orientation of the yield zone. These results indicate that, assuming the stress state is such that slip of joints will occur, the yield behavior of the rock mass is probably more sensitive to orientation than spacing. The anisotropy seen here is a result of a similar phenomenon to that seen by Graziev and Erlikhman (1971) when examining pressure "bulbs" (lines of equal pressure from model tests) beneath footings on bedded materials. Figure 26 shows the effects of primary joint orientation on the pressure distribution in the foundation. The stress tends to orient itself at right angles to the structure as a result of slip. For structures oriented at low angles to the applied stresses, joint slip can result in highly anisotropic stress fields.

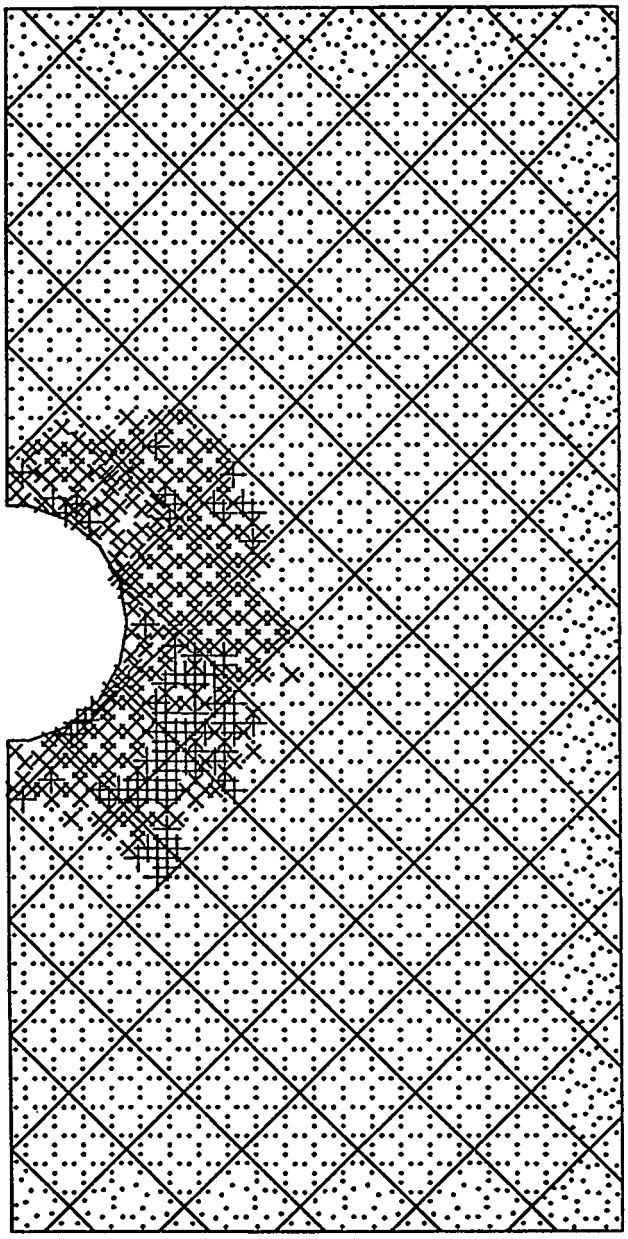

Fig. 23 Yield Zone Around a Circular Tunnel for Joints Oriented at ±45° and S/a Ratio of 0.333

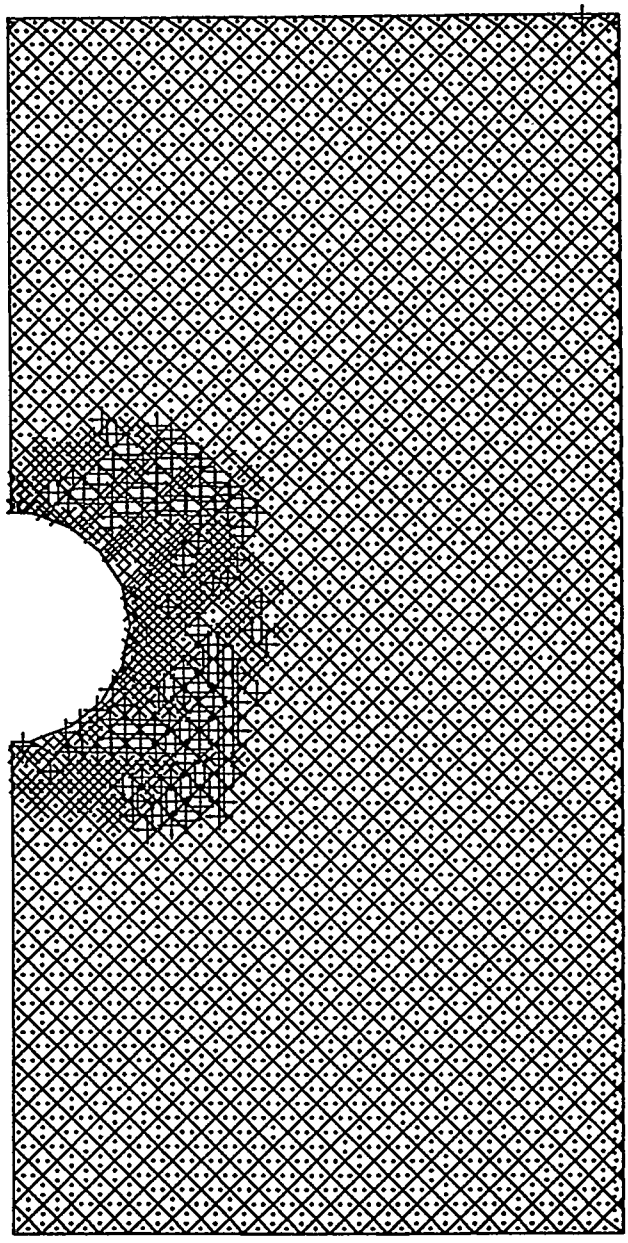

Fig. 24 Yield Zone Around a Circular Tunnel for Joints Oriented at ±45° and S/a Ratio of 0.083

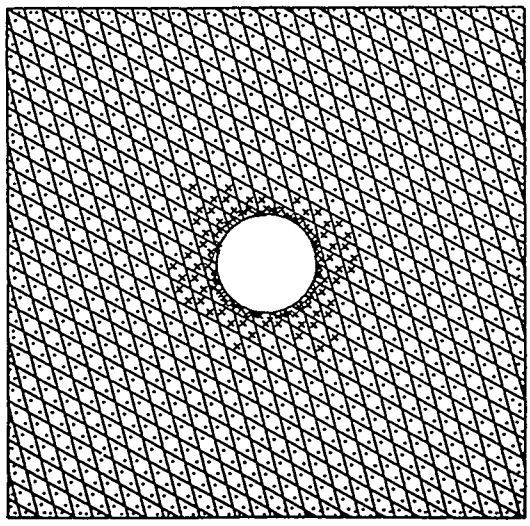

(a)

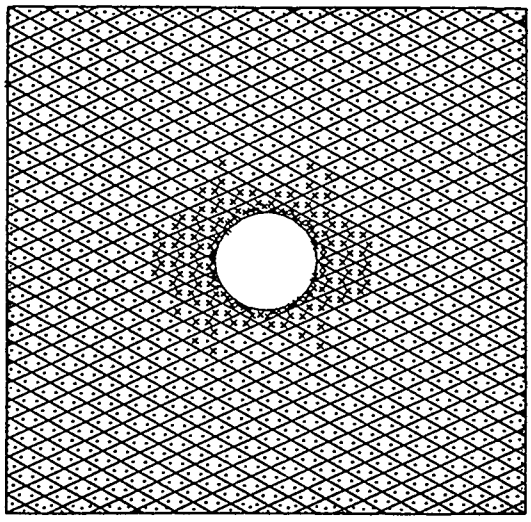

(b)

Fig. 25 Yield Zones Around a Circular Tunnel for Joints Oriented at (a) -15°/-70° and (b) 65°/-60° for the S/a Ratio of 0.167

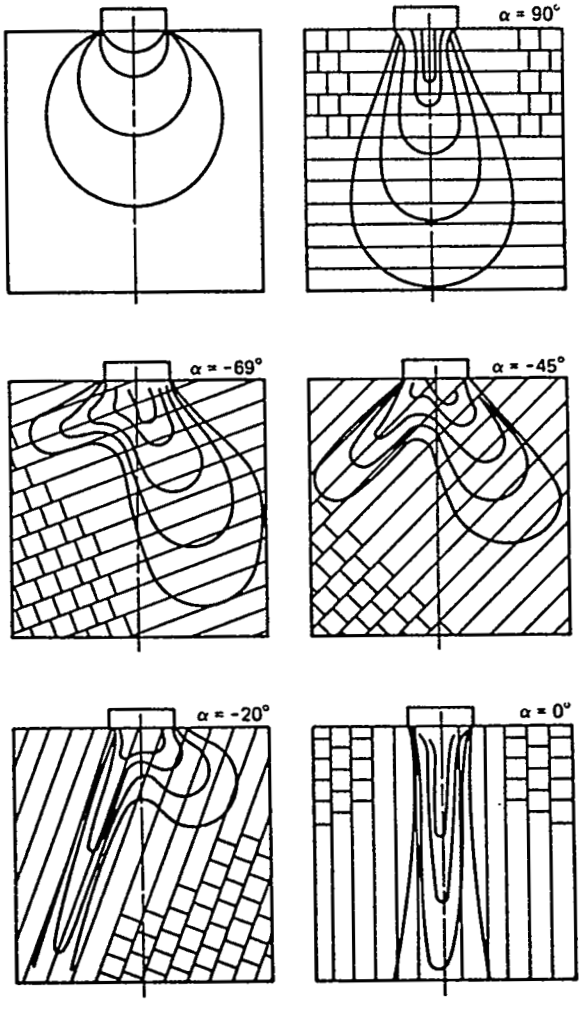

Fig. 26 Lines of Equal Stress (Bulbs of Pressure) Determined by Gaziev and Erlikhman [1971] From Models

The spacing of joints will control, to some extent, the failure mechanisms. For large joint spacings ($S/a > \approx 0.5$), wedge failures dominated by rotation of blocks will occur. For small ratios of S/a (< 0.1), failure representing continuum yield will occur. Combinations of continuum failure and wedge failure resulting from joint slip will also occur.

The final category, Model 6, regards isolated fractures, such as faults, in the rock mass. These fractures may intersect an opening or may be isolated from excavations. Questions of concern here may include mining- or thermally-induced fault slip. In general, this type of problem is restricted to discontinuum methods or continuum models with interface elements.

Examples are presented later which illustrate the use of continuum and discontinuum methods as they apply to wste disposal problems in welded tuff.

3.0 THE YUCCA MOUNTAIN SITE

3.1 Geographic Setting

The Yucca Mountain Site is located in Southern Nevada, roughly 150 km north and west of Las Vegas, on land controlled by the U.S. Air Force, the U.S. Department of Energy (DOE), and the Bureau of Land Management (Fig. 27).

Yucca Mountain lies in the Great Basin, a sub-province of the basin and range province. Yucca Mountain is an irregularly-shaped volcanic upland with elevations of about 1500 to 1930 m at the crest, with about 650 m of relief. The mountain is composed of eastward-dipping volcanic and volcaniclastic strata broken into echelon fault blocks (MacDougall et al., 1987).

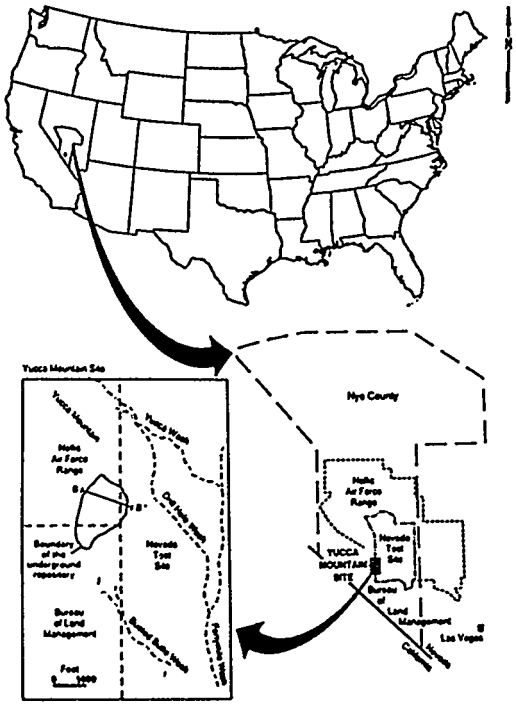

Fig. 27 Location Map for Yucca Mountain Site [U.S. DOE, 1988(b)]

3.2 Stratigraphy and Lithology

Figure 28 shows a stratigraphic section taken North-South across Yucca Mountain produced by geologic correlations between drill holes. The rocks comprising Yucca Mountain are a 300-1000 meters thick sequence of tertiary silicic volcanic rocks consisting of a series of welded and non-welded ash-flow and ash-fall tuffs and lavas and volcanic breccias. The volcanic rocks at Yucca Mountain comprise seven formations, each containing several members differentiated on the basis of lithologic or physical and chemical properties or both. The units are laterally continuous and vary in thickness from 70 to approximately 370 meters.

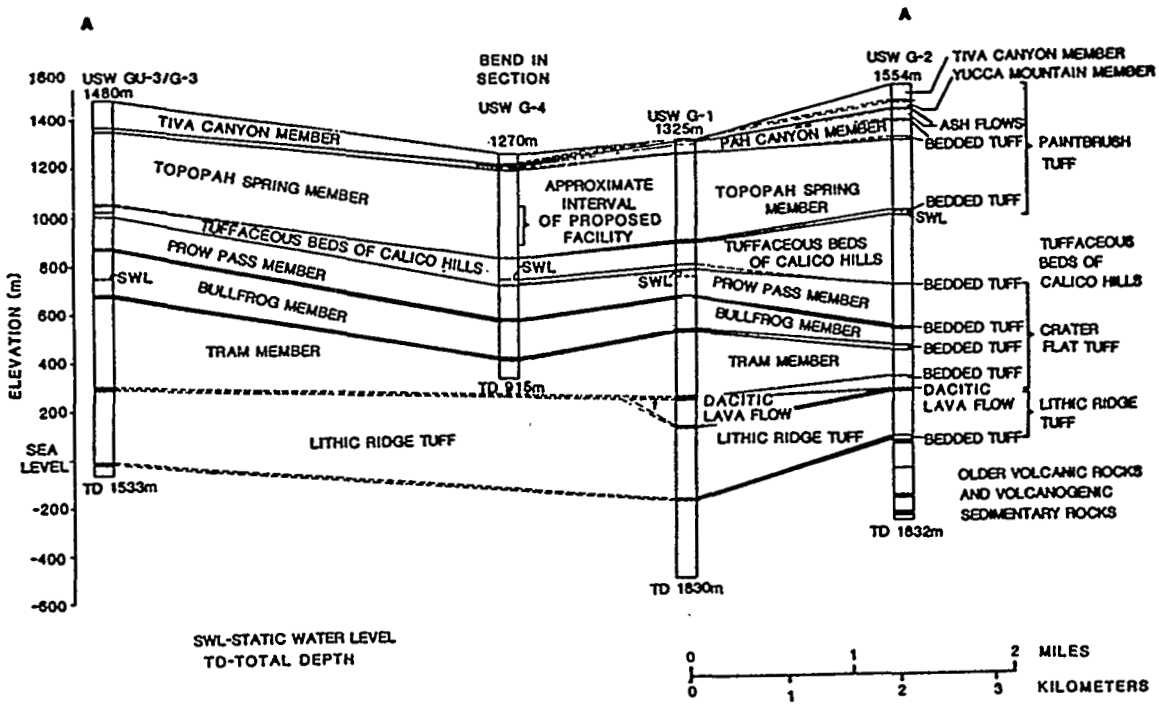

Fig. 28 North-South Cross-Section of Yucca Mountain Site from Drill Hole Correlation [MacDougall et al., 1987]

Rock being considered for a repository at Yucca Mountain is the densely welded ash-flow tuff of the Topopah Spring Member, a multiple flow unit of the Paintbrush Tuff, as shown in Fig. 28. The following description of the Topopah Spring flow is taken from the CDSCP (U.S. DOE, 1988(a), p. 1-62): a non-welded to partially-welded glassy basal zone, from 10 to 20 meters thick, grades upward by increased welding into a densely-welded basal vitrophyre from 10 to 25 meters thick. The basal vitrophyre grades abruptly upward into a densely welded, devitrified, unvesiculated zone, the lower non-lithophysal zone, from 27 to 56 meters thick. This zone grades upward into the lower lithophysal zone, from 43 to 117 meters thick. Overlying the lower lithophysal zone is the middle nonlithophysal zone, from 54 to 96 meters thick, representing the vesiculated portion of the second eruptive phase. Finally, a third eruptive pulse of quartz-latitic ash-flow tuff forms the caprock zone, from 39 to 62 meters thick. A thin (approximately 1 m) vitrophyre, occurring in most places in the uppermost part of the caprock, resulted from chilling at the upper surface of the ash flow. The proposed repository horizon lies within the lower non-lithophysal zone in the lower part of the member. This zone, 27 to 56 meters thick, is rhyolitic, devitrified, and moderately to densely welded. The percentage of lithophysae ranges from 0 to 2 percent.

3.3 In-Situ Stress State

Stress measurements have been conducted by hydraulic fracturing in exploration holes drilled within the Yucca Mountain Site. These are supplemented by past overcoring and hydraulic fracturing measurements in Ranier Mesa. The mean values and ranges are given in Table 1.

Table 1

MEAN VALUES AND RANGES FOR PRINCIPAL STRESSES
[MacDougall et al., 1987, Chapter 6, Table 6-10]

Parameter	Mean Value*	Range
σ_v (MPa)	7.0	5.0 to 10.0
σ_{hmin}/σ_v	0.55	0.3 to 0.8
Bearing of σ_{hmin}	N57°W	N57°W to N65°W
σ_{hmax}/σ_v	0.65	0.3 to 1.0
Bearing of σ_{hmax}	N32°E	N25°E to N40°E

* mean value at depth of approximately 300 meters

3.4 Rock Properties for the Topopah Springs Formation

The rock mass can be divided into the intact rock mass and the discontinuities. Formulation of a continuum or discontinuum constitutive model requires properties and constitutive relations of both.

3.4.1 Intact Rock

The intact rock properties of importance here include the stiffness, strength and thermal properties. Table 2 provides a summary of the pertinent properties.

Table 2

INTACT ROCK MECHANICAL AND THERMAL PROPERTIES OF THE TOPOPAH SPRINGS (TSW_2) [MacDougall et al., 1987, CDSCP, Chapter 6]

Property	Average Value	Range
Young's Modulus (GPa)	30.4	± 6.3
Poisson's Ratio	0.24	± 0.06
Uniaxial Compressive Strength (MPa)	166.0	±65.0
Cohesion (MPa)	34.0	±11.4
Friction Angle (deg)	23.5	± 0.15
Tensile Strength (MPa)	15.2	
Thermal Conductivity (W/m°C)	1.84	± 0.12
Coefficient of Thermal Expansion (/°C)	8.8×10^{-6}	
Thermal Capacitance (J/cm^3K)	2.16	

3.4.2 Jointing in the Topopah Spring

In most instances, the properties and geometry of the joints controls the strength and failure modes of the rock mass. The primary properties of interest include the cohesion and friction angle of the joint surfaces and their spacing and continuity. Table 3 gives properties of joints for the non-lithophysal Topopah Springs formation.

Table 3

JOINT PROPERTIES
[MacDougall et al., 1987, CDSCP, Chapter 6]

Property	Value		
	UB	RV	LB
Shear Stiffness (MPa/m)	10^7	10^6	10^5
Joint Cohesion (MPa)	0.2	0.1	0
Friction Angle (deg)	38.7	28.4	11.3
Residual Friction Angle (deg)	38.7	28.4	11.3
JCS	113.0	171.0	229.0
JRC	12.0	9.0	6.0

UB = upper bound
RV = recommended value
LB = lower bound
JCS = joint wall compressive strength (NGI classification)
JRC = joint roughness coefficient (NGI classification)

The fracture frequency in fractures per meter for various angles of inclination (in degrees downward from horizontal) is presented in Fig. 29. The data for this plot was derived from two surface drill holes (MacDougall et al., 1987, CDSCP, Chapter 6, Table 6-15). The figure shows a large number of sub vertical fractures present in the repository horizon with an average spacing of about 8 mm, but no other discernible sets. Because the counting of fractures in drill holes tends to bias the results away from fractures sub-parallel to the hole axis, these results may not be completely reliable; however, they indicate a strong vertical preferential jointing orientation.

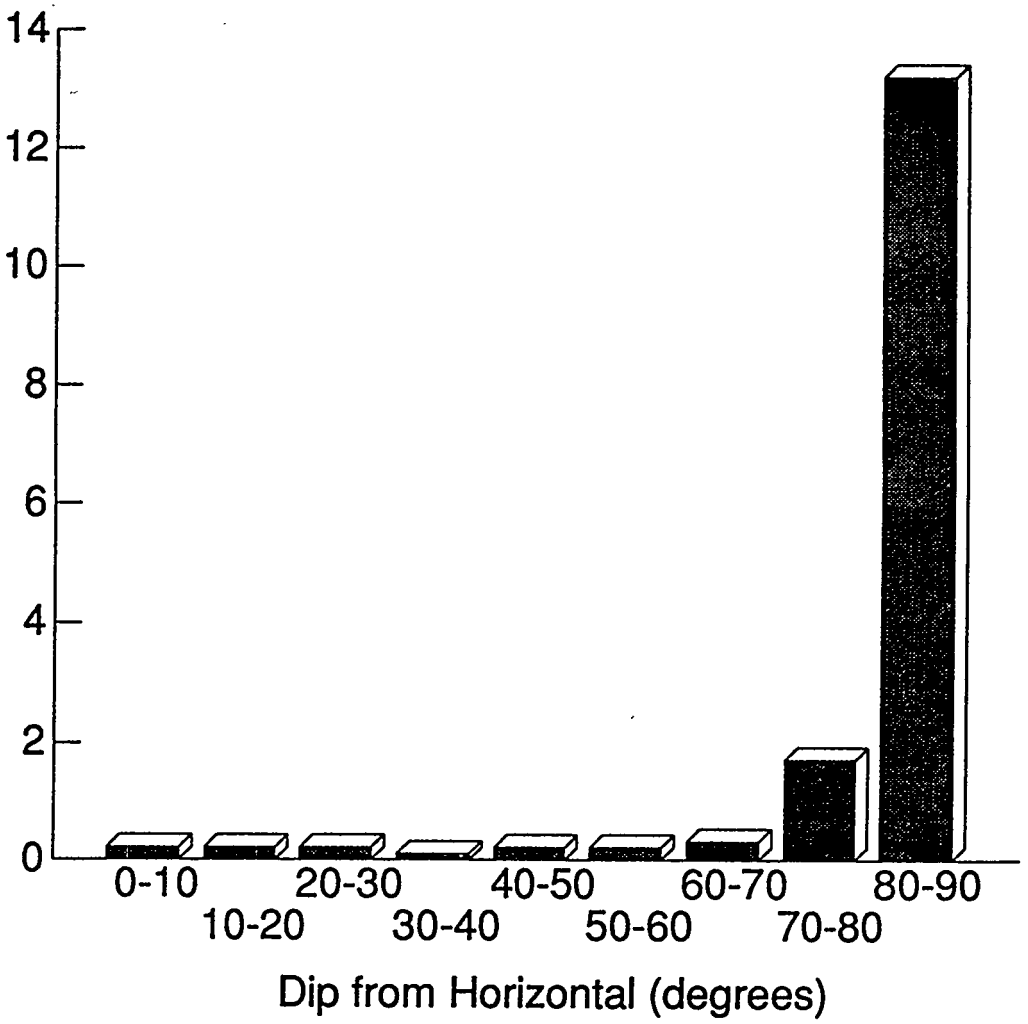

Fig. 29 Fracture Frequency in the Topopah Springs Formation as a Function of Angle of Inclination Downward from Horizontal [Data from four vertical boreholes from MacDougall et al., 1987, CDSCP, Chapter 6]

3.5 Rock Mass Properties

Several in-situ tests have been conducted in the G-Tunnel facility in the Grouse Canyon welded tuff for determination of large scale or "rock mass" properties. These tests include the Small Diameter Heater Experiment [Zimmerman et al., 1986(a)] and the Heated Block Experiment [Zimmerman et al., 1986(b)]. The results of these tests showed that fracturing has little effect on the thermal properties of the rock mass and that laboratory-determined thermal properties are sufficient for design. The heated block experiment was used to determine equivalent elastic properties for the rock mass. A 2 m by 2 m by 2 m cube of welded tuff was biaxially compressed by flatjacks as displacements of the block were measured. Based on these measurements, the design value for deformation modulus was reduced by 50% to 15.2 GPa ± 4.2 GPa. The Poisson's Ratio, however, is estimated to be the same as the intact value. These estimates of in-situ properties were made by fitting a straight line to field loading data.

The strength properties (uniaxial compressive strength, cohesion, friction) of the rock mass were determined simply from personal judgment by reducing the uniaxial compressive strength by 50%. There is no specific theoretical or field justification given for these values.

3.6 Faults in the Near Vicinity of the Yucca Mountain Site

The structural geology of the area in and around the Yucca Mountain site is complex. One expression of this complex structure is the faulting of the silicic tuffs composing Yucca Mountain. Two phases of faulting are identified in the Site Characterization Plan (SCP) [U.S. DOE, 1988(b)]: (1) older extensional faulting associated with silicic volcanism from about 11 to 7 million years ago; and (2) basin-and-range faulting for about the past 7 million years. Yucca Mountain is a series of north-trending structural blocks that have been tilted eastward along west-dipping, high-angle normal faults. The proposed repository is to be excavated in a block which dips eastward at 5° to 10°. The block is bounded on the west by the Solitario Canyon fault, on the northeast by the Drill Hole Wash structure, and on the east and southeast by the western edge of the Imbricate normal fault zone. One known fault, the Ghost Dance fault, transects the central portion of the proposed repository area in, roughly, a north-south fashion. Figure 30 is a plan view of the area around Yucca Mountain showing the surface locations of faults. Figure 31 shows an east-west section across the northern portion of the proposed repository block illustrating the location of faults with respect to the repository horizon.

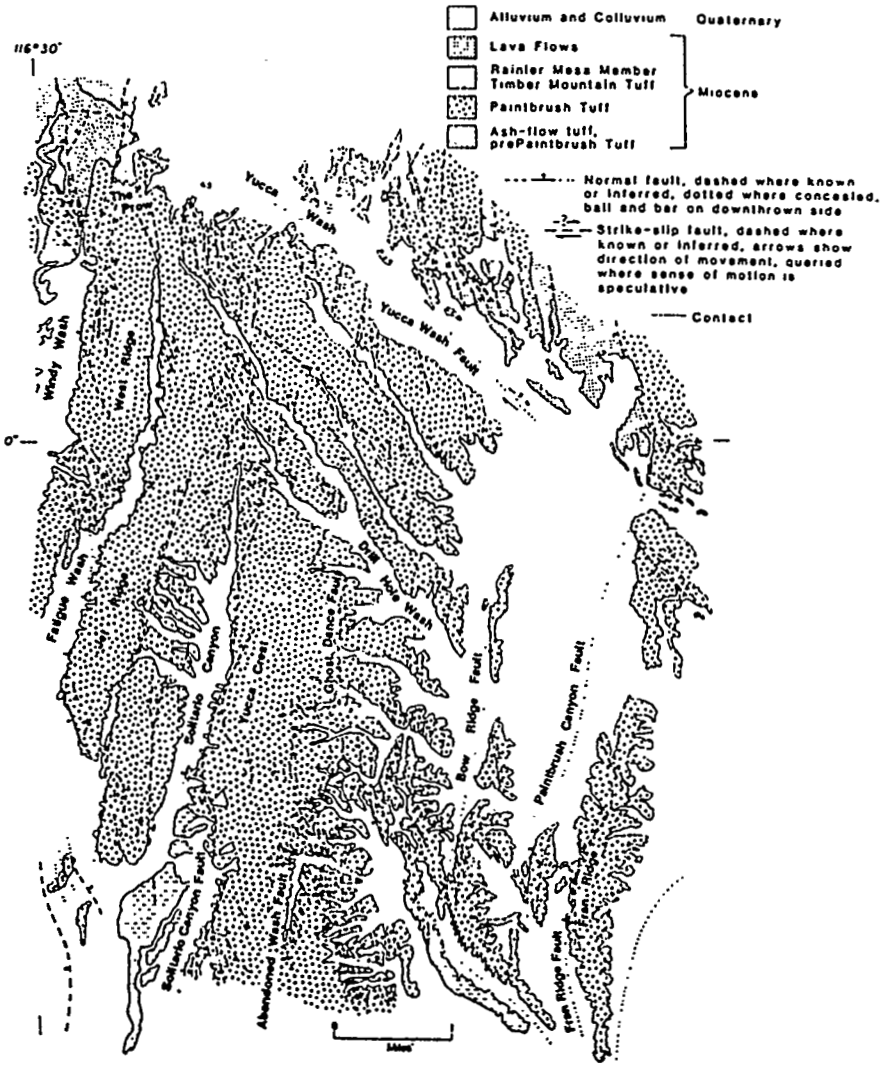

Fig. 30 Faults in the Vicinity of Yucca Mountain [U.S. DOE, 1988(b)]

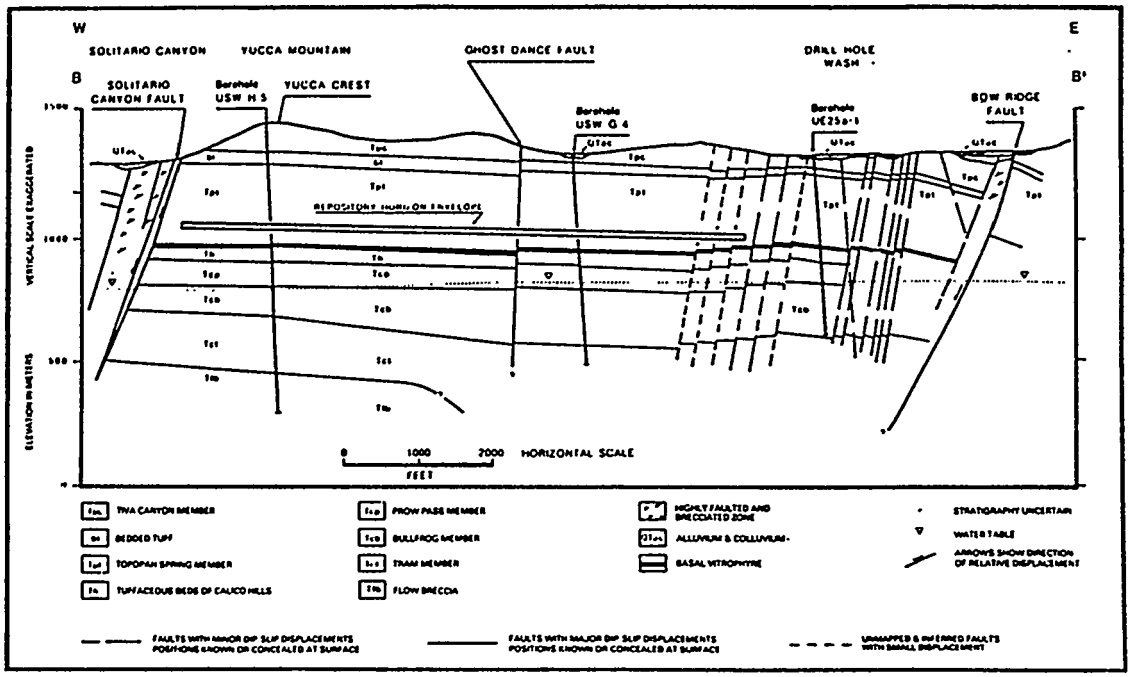

Fig. 31 East-West Geologic Cross-Section for the Yucca Mountain Site. This figure shows the relative positions of various tuff units at the site, including the unit proposed for the repository, and the fault zones that are closest to the site. [U.S. DOE, 1988(b)]

Vertical offsets of these fault structures have been measured. Most of the structures reportedly show offsets of 15 feet or less, with the exception of the Ghost Dance and Solitario Canyon faults. The Ghost Dance fault shows an offset of 38 meters at the southeast end of the repository area. The Solitario Canyon fault shows offsets ranging to 213 meters at the northwest corner. Quarternary movement reportedly is seen on the Windy Wash, Solitario Canyon, Bow Ridge, Paintbrush Canyon and Bare Mountain faults in the vicinity of the Yucca Mountain site [U.S. DOE, 1988(b)].

Seismic records from the past 150 years (including recent seismic monitoring) show the Yucca Mountain area to be relatively quiet seismically [U.S. DOE, 1988(b)]. It has not been possible to correlate seismicity with specific faults or structures. DOE's current estimates for the seismic design is based on a full-length rupture on the Bare Mountain fault, resulting in a magnitude 6.8 earthquake with expected peak ground acceleration of 0.4 g.

Geoengineering questions which currently remain regarding fault structures at Yucca Mountain are their effects on stability of the underground openings, their stability under seismic loading from earthquakes and/or nuclear testing at the Nevada Test Site, and their stability under thermally-induced loads. Also of potential importance, but beyond the scope of this discussion, is the influence of faulting on water movement through the beds over- and underlying the repository horizon.

3.7 Summary

At present, the structure of the Topopah Springs at the repository location is know only from surface-based diamond drill holes. In the SCPCDR [McDougall et al., 1987] and the SCP [U.S. DOE, 1988(b)], and their supporting documents, there is no consistent definition of the mechanical constitutive model presently in use for performance assessment and design. In various locations, the rock is considered to be an elastic (with use of the Hoek-Brown empirical criterion), Mohr-Coulomb or compliant joint material. There does appear to be a general consensus that the rock mass can be treated as a homogeneous linear thermal material with conductive heat transfer mechanisms in the rock mass. A significant amount of laboratory and in-situ thermal and mechanical testing has been performed. Most of this testing has been directed toward intact rock, with few tests of natural joints. The compliant joint models suggested for use in performance assessment in many NNWSI documents require detailed information on the initial aperture and mechanical behavior of joints. Much of the required data for these models has yet to be gathered.

4.0 SELECTION OF MODEL TYPES FOR THE YUCCA MOUNTAIN SITE

4.1 Model Geometric Scale

The choice of continuum versus discontinuum modeling approach and constitutive model type suitable for use at Yucca Mountain depends heavily on the geometric scale of the analyses to be performed. Three general scales of analysis have been used for repository thermomechanical modeling:

(1) canister scale — includes detailed studies of the response of the canister borehole, liner, and the intersection of the hole to the emplacement room;

(2) room scale — includes determination of the stability of the emplacement rooms and the region within about 10 room diameters surrounding them. At this scale, the canisters are usually represented by line or multiple point heat sources.

(3) regional scale — includes analysis of the thermomechanical effects of the repository on the rock mass surrounding the repository to the ground surface. This may include an analysis of disturbed zone, stability of service structures such as shafts and ramps, fault stability and its effects on performance, and possible thermal convective mechanisms for groundwater transport.

As the geometric scale of the analyses changes, the scale of the features of importance changes as well. Table 4 summarizes the dimensions of openings in relation to the physical scale of rock structure at each of the analysis scales. Using the approach of Starfield and Detournay described previously, a model type is suggested for each analysis scale.

Table 4

MODEL TYPE FOR VARIOUS ANALYSIS SCALES

Analysis Scale	Principal Excavation Radius, a (m)	Fracture Spacing, S* (m)	S/a	Suggested Modeling Approach
canister	canister borehole a = 0.37	jointing, S: = 0.07 - 0.1	= 0.25	compliant joint: possibly distinct element to examine liner loading from wedge failure
room	emplacement room, vertical emplacement a = 3 m (average) set)	jointing, S = 0.07 p 0.1 (major vertically-oriented	= 0.03	continuum model: anisotropic plasticity, such as ubiquitous joint or compliant joint. Elastic model with in-situ modulus reduction may work, depending on joint friction, cohesion.
regional	repository, 1000's of meters	faults treated treated as discrete features		discontinuum: faults must be treated as discrete features; includes (i) distinct element, (ii) interface elements in continuum code;

*For all scales, the possibility exists for a continuous, through-going structure (fault) to shafts and ramps (see room-scale analysis).

4.2 Canister Scale

For the canister scale, the principal excavations of concern are the emplacement boreholes. The physical scale of the analysis is the near field surrounding a borehole and, mechanically, includes roughly 10 borehole radii. The principal structural feature at this scale is the jointing which, from site characterization studies to date, has a primary vertical orientation. The ratio of joint spacing, S, to the radius of the borehole, a, is approximately 0.25.

Of greatest importance at the canister scale is the ability of the rock mass to dissipate the heat generated by the waste and the stability of the boreholes. Present vertical emplacement designs (MacDougall et al., 1987) call for a lining only in the upper portions of the emplacement hole. Therefore, even small amounts of debris resulting in failure of wedges in the walls of the holes can create difficulty in retrieval of the canisters. A method is necessary which can examine the potential for wedge-type failure of the hole and the loading of the canister (or liner, if present). Since local geology will play such an important role in hole stability, it is questionable how representative any model will be in examining this problem. The models can, however, provide some insight into the extent of failure under the potential best and worst conditions. A compliant joint type model may provide insight into the extent of failure—i.e., whether a problem exists or not. Detailed examination of decrepitation mechanisms and possible loading of the liner would appear to be restricted to a large deformation discontinuum approach.

4.3 Room Scale

Sample analyses of emplacement room response to vertical emplacement of waste over the proposed retrieval period were given by Brandshaug (1989). A ubiquitous joint model was used to represent the Topopah Springs formation with intact rock and joint properties and in-situ stress state taken from the CDSCP [U.S. DOE, 1988(a)]. The ubiquitous joints were assumed to be oriented vertically with a friction angle of 28° and cohesion of 0.1 MPa. A commingled array of spent fuel and defense high-level waste was assumed to be placed vertically with an initial power of 3.2 kW/canister for spent fuel and 0.42 kW/canister for DHLW. Spacings of the waste canister were as given in Chapter 4 of the SCPCDR (MacDougall et al., 1987) to create an overall gross thermal loading of 57 kW/acre. Regions of joint slip are predicted for excavation only, and for 50 years after waste emplacement.

Figures 32-34 show areas of predicted joint slip and contours of the stress state after excavation and joint slip regions just prior to and following retrieval. Regions of slip are confined to within about one radius of the emplacement room, and are confined primarily to the room corners and walls. There is very little additional slip as a result of heating. The closure of the room (Fig. 35) does not indicate instability, and is little more than those expected from elastic response of the rock only.

The prediction of the extent of yield in the rock mass is highly sensitive to the value chosen for cohesion. In the range of joint properties given in the SCP [U.S. DOE, 1988(a)], the friction angle can vary from approximately 11° to 39°, and cohesion from 0.0 to 0.2 MPa. Christianson (1989) examined the effect of this range of properties on the response of disposal rooms to vertical emplacement for the same waste properties and loading density as in the SCPCDR. For the case of 11° friction and 0 MPa cohesion, the yield zone at 50 years is far more extensive (over 2 diameters), yet the system is not unstable, and displacements are within the design criteria established in the SCPCDR (See Fig. 36). These runs indicate that, over the range of properties given, and assuming a single vertical joint set, instability of the openings is probably not a great concern over the entire retrieval period. It is estimated that only light support, including bolts and wire mesh, is required. It is noted, however, that these calculations are based on the assumption of a single set of closely-spaced vertical joints. Experience with continuum joint models has shown that stability of the openings is very sensitive to the number and attitude of joints sets. If the above simulations were performed using an isotropic plasticity formulation (i.e., a standard Mohr-Coulomb type model), completely different yield patterns would be seen, and unstable deformations would result for a cohesion of zero.

For the room-scale analyses, it would appear that a continuum model can be used, but a constitutive law consistent with the structure of the Topopah Springs is probably a ubiquitous or compliant joint model. The results given in Brandshaug (1989) indicate that, for the average laboratory-determined Topopah Springs properties, and the assumed vertical joint orientation, that the rock mass deformations are not significantly different than would be provided by an elastic model. The results of the model may change significantly, however, if number and attitude of the joint sets are changed. The applicability of the model ultimately will be determined from underground site characterization and comparison to instrument data form the ESF.

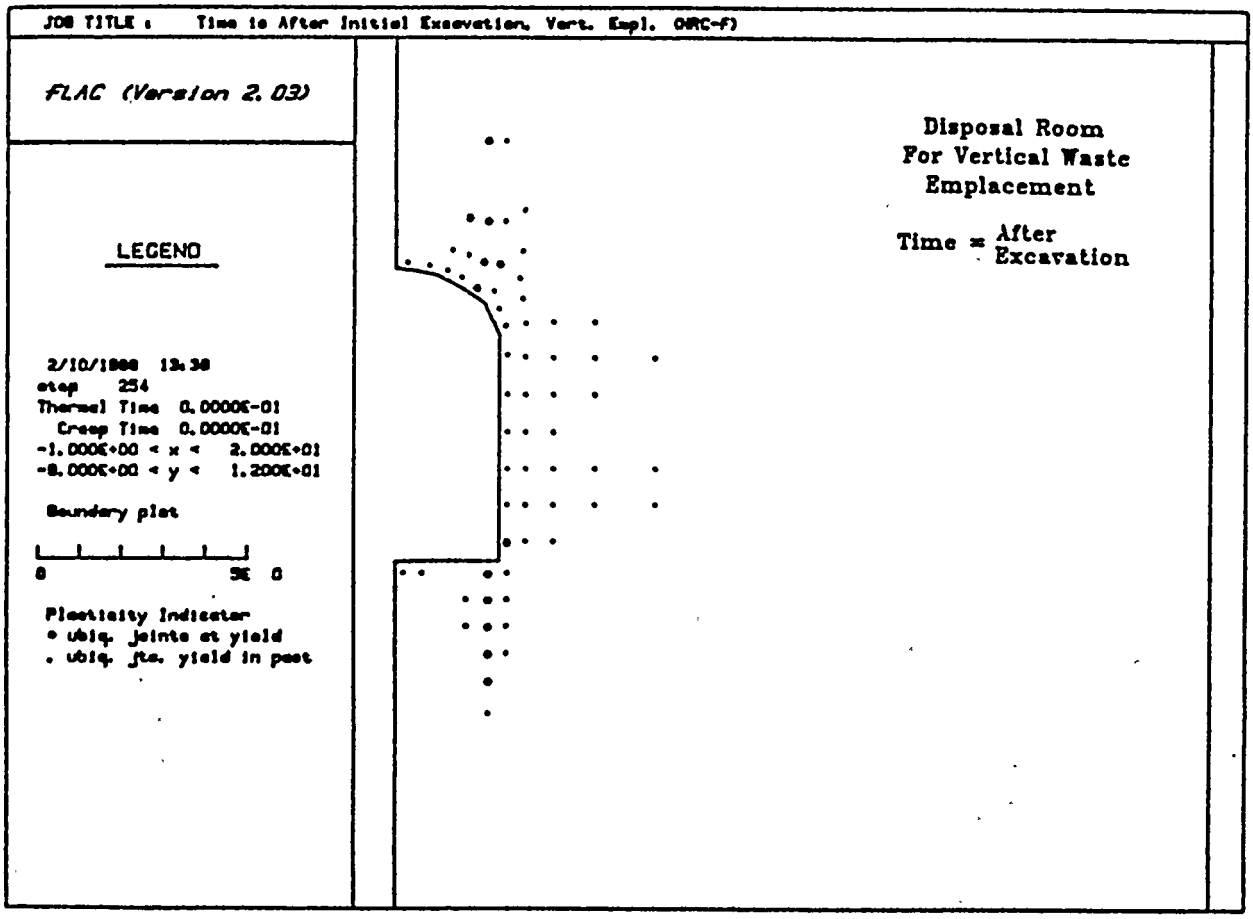

Fig. 32 Predicted Slip Along Vertical Joints as a Result of Excavation of the Waste Disposal Room for Vertical Emplacement [Brandshaug, 1989]

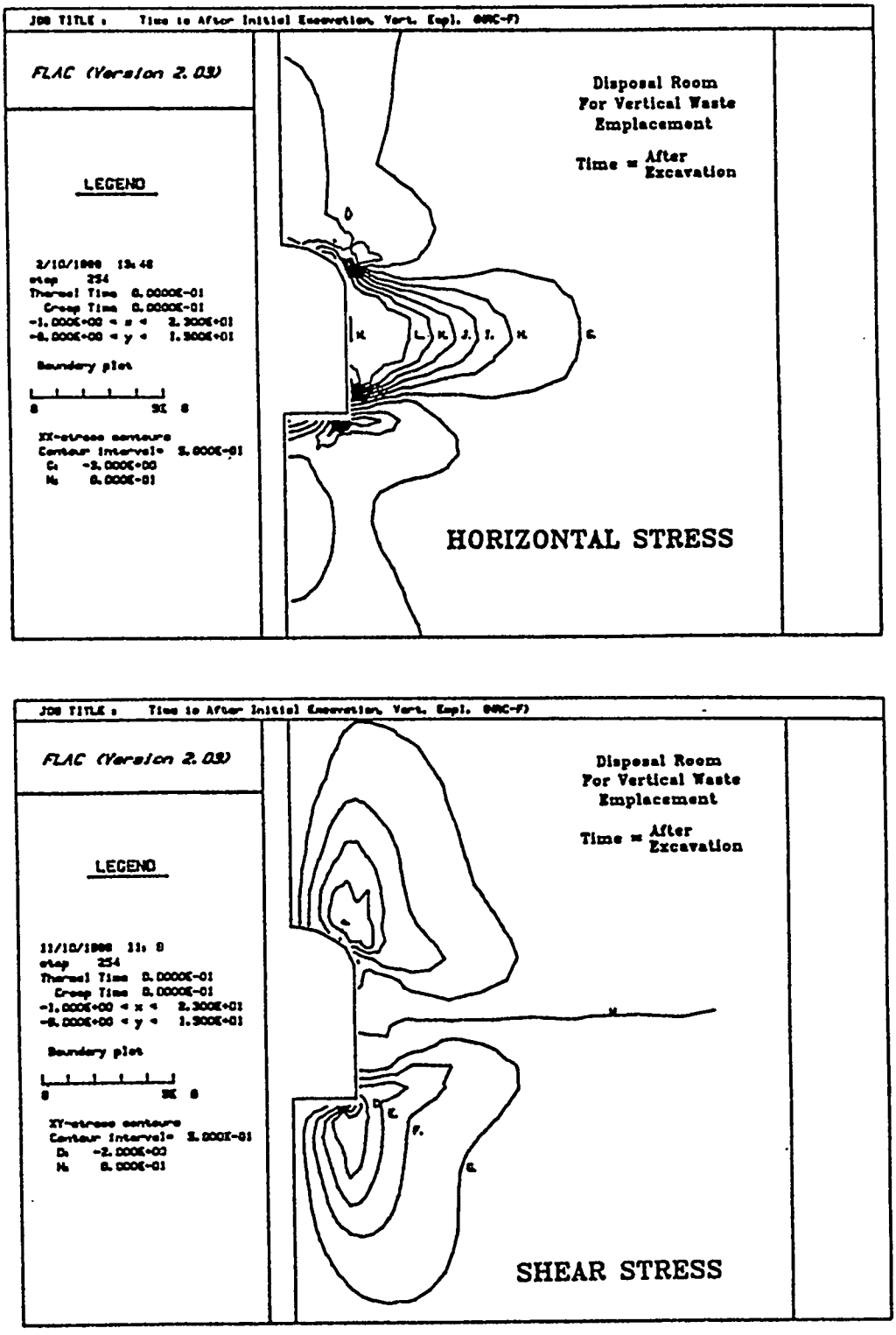

Fig. 33 Predicted Shear and Horizontal Stresses as a Result of Excavation of the Waste Disposal Room for Vertical Emplacement [Brandshaug, 1989]

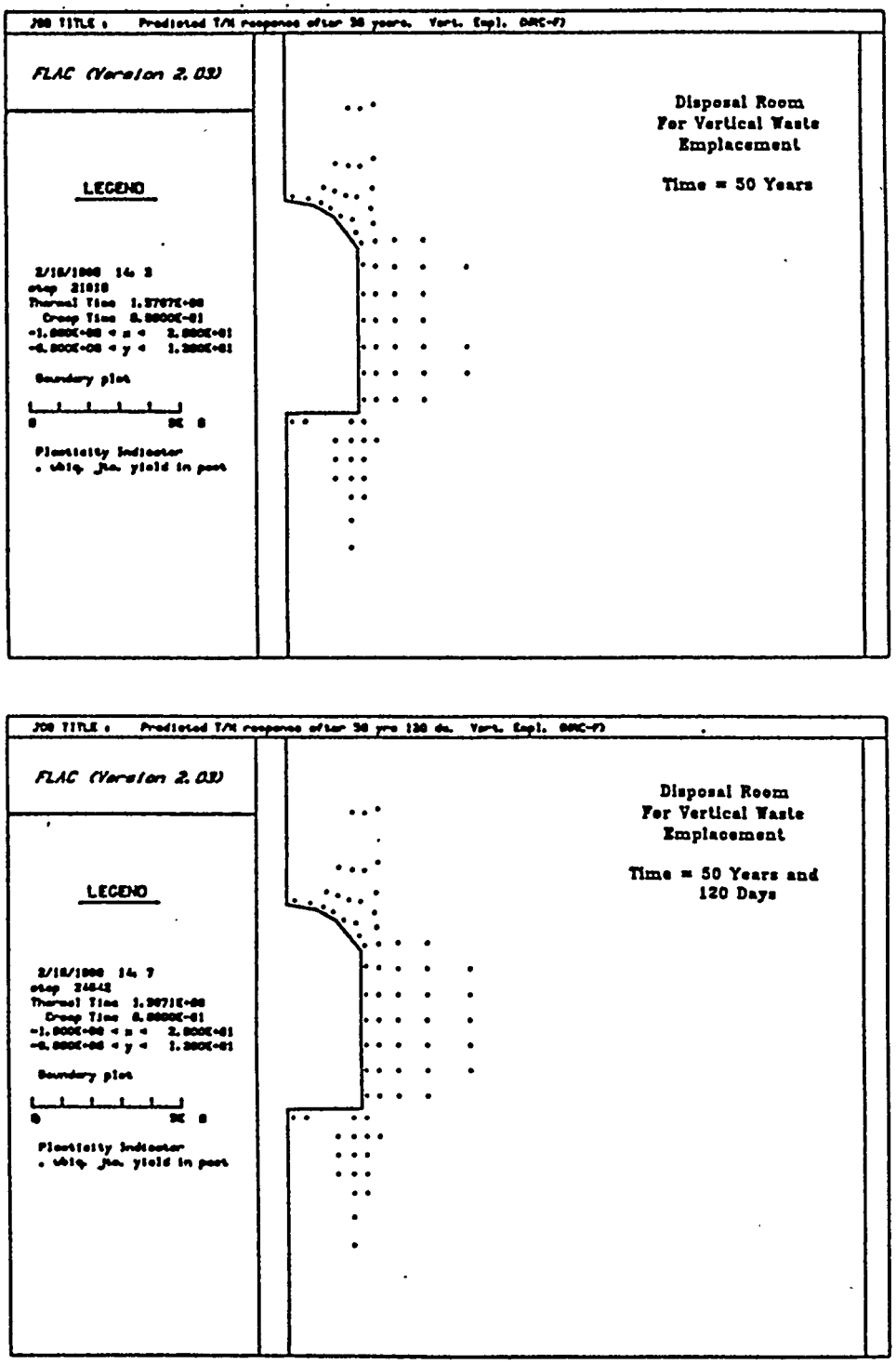

Fig. 34 Predicted Slip Along Vertical Joints Around the Waste Disposal Room for Vertical Emplacement at the Time of Waste Retrieval and After Waste Retrieval [Brandshaug, 1989]

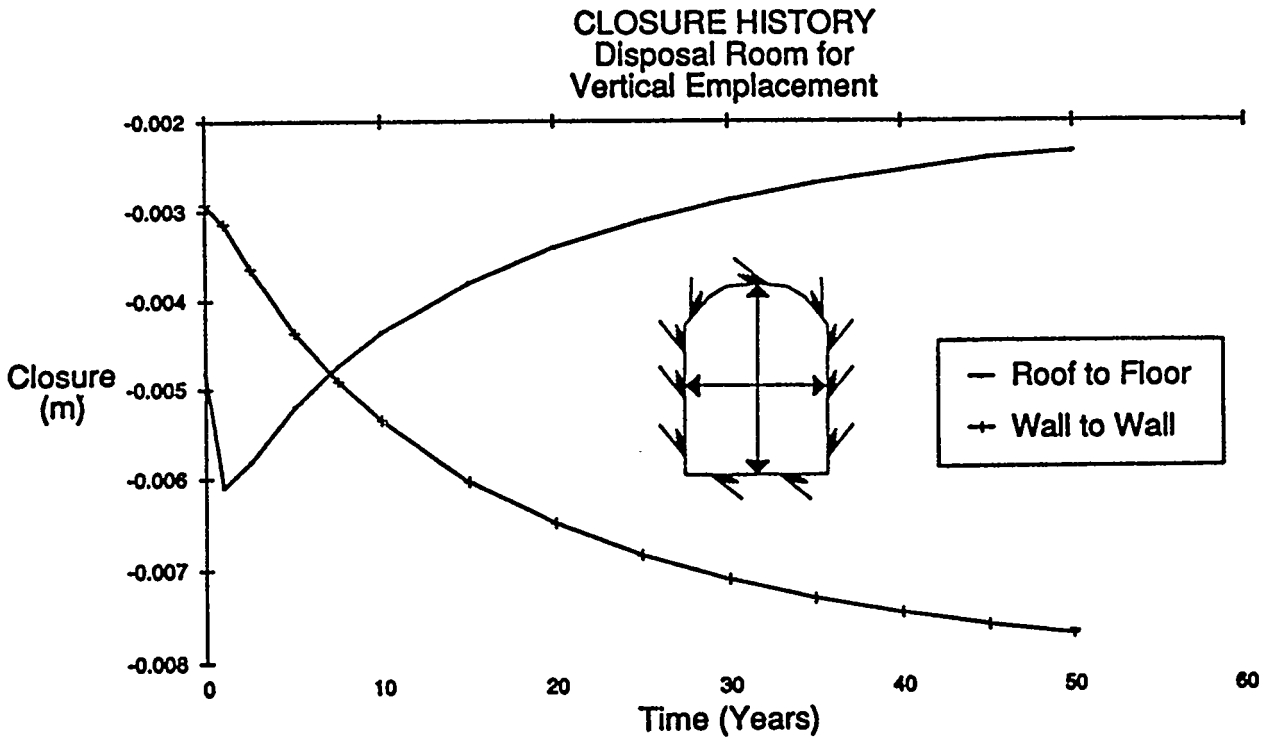

Fig. 35 Predicted History of the Roof to Floor Closure and Wall to Wall Closure of the Waste Disposal Room for Vertical Emplacement [Brandshaug, 1989]

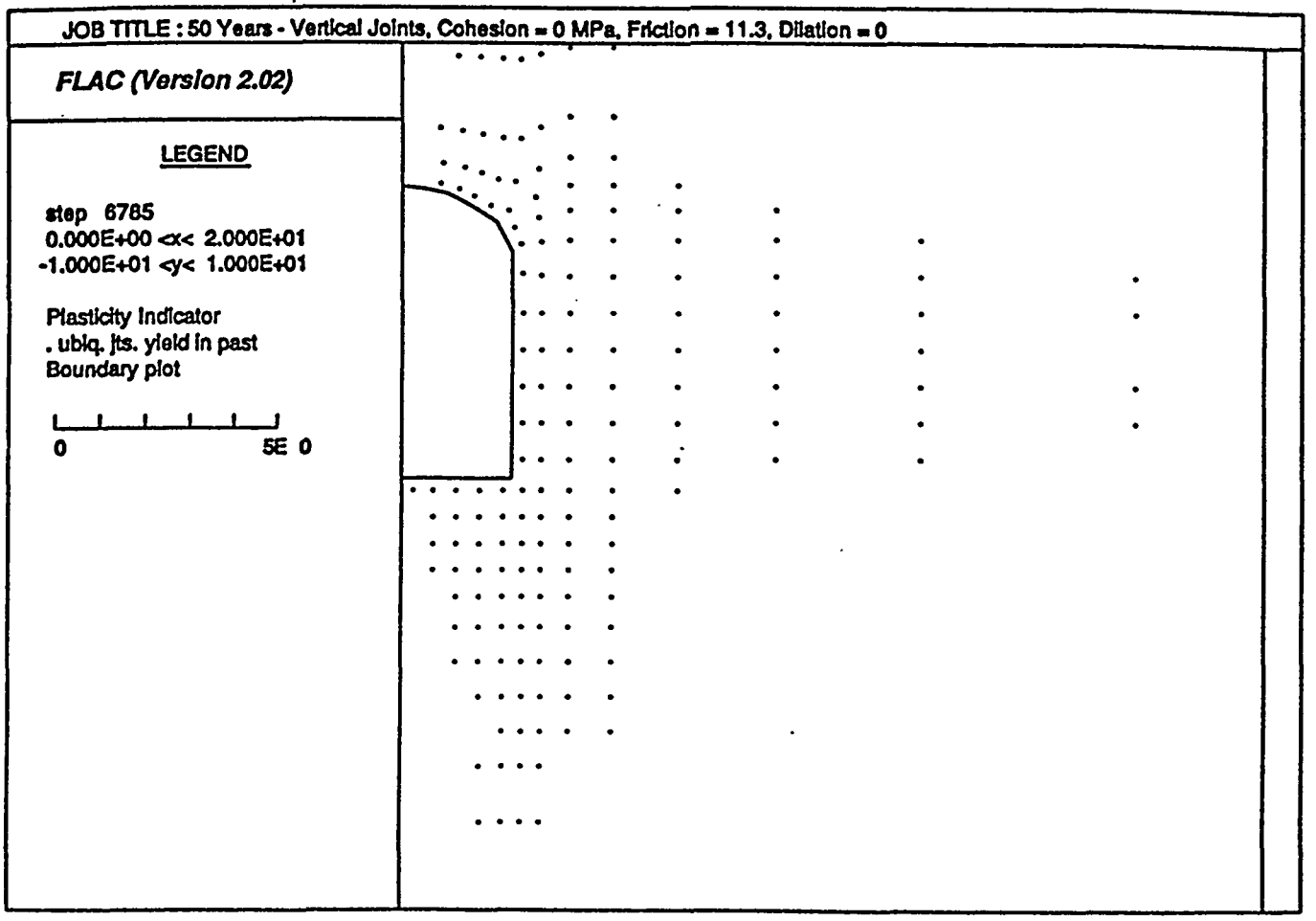

Fig. 36 FLAC Joint Displacements for 50 Years (vertical joints, cohesion = 0 MPa, friction = 11.3, dilation = 0) [Christianson, 1989]

4.4 Regional Scale

The regional-scale modeling pertains primarily to performance assessment studies involving radionuclide transport. Inherent in the discussion of performance assessment is the estimation of thermomechanical disturbance to the surrounding rock mass. A commonly accepted definition of the disturbed zone or its impact on fluid transport in an unsaturated rock mass has not been established. The regional-scale models can provide some insight as to the thermal and mechanical effects in the far field resulting from waste disposal. In the regional scale, model dimensions are of the order of thousands of meters. The non-linear response of the rock mass directly surrounding an opening is of little importance, and the excavation itself is not modeled. Heat sources often are modeled as point sources which are "smeared" out across the repository plane to provide the correct gross thermal load. At this scale, joints cannot be taken into account explicitly, but their effects may be examined empirically. Mack et al. (1989) have examined the extent of mechanical and thermal disturbance around a repository at Yucca Mountain using the thermoelastic boundary element program HEFF (Brady, 1988). Although HEFF does not simulate inelastic rock behavior associated with opening or slip on jointing in the far field, a first-order engineering estimate of the extent of joint opening and slip were inferred by using empirical equations describing the joint deformation under normal and shearing stresses (Bandis et al., 1983). The potential slip and aperture changes can then be calculated and related to their effects on fluid transport through the medium. Figures 37 to 39 show regions in which the apertures of vertically-oriented joints have increased or decreased by a factor of two or more for 25, 100 and 500 years after waste emplacement. A ratio of vertical-to-horizontal stress of 1.67 was used in these runs with a gross thermal loading of 80 kW/acre. Regions of induced slip on vertical joints for the same case are shown in Figs. 40 to 42. These plots indicate significant mechanical disturbance to the joints extending to the ground surface. This is a result of the thermally-induced tension which exists around the repository at increasing radial distance with time. The effect of joint aperture increase, or joint slip in an unsaturated medium where matrix flow may dominate [U.S. DOE, 1988(b)] fluid flow is not examined in the study by Mack et al. (1989). This type of question will need to be addressed, however, in the license review process and may require similar forms of regional scale analyses.

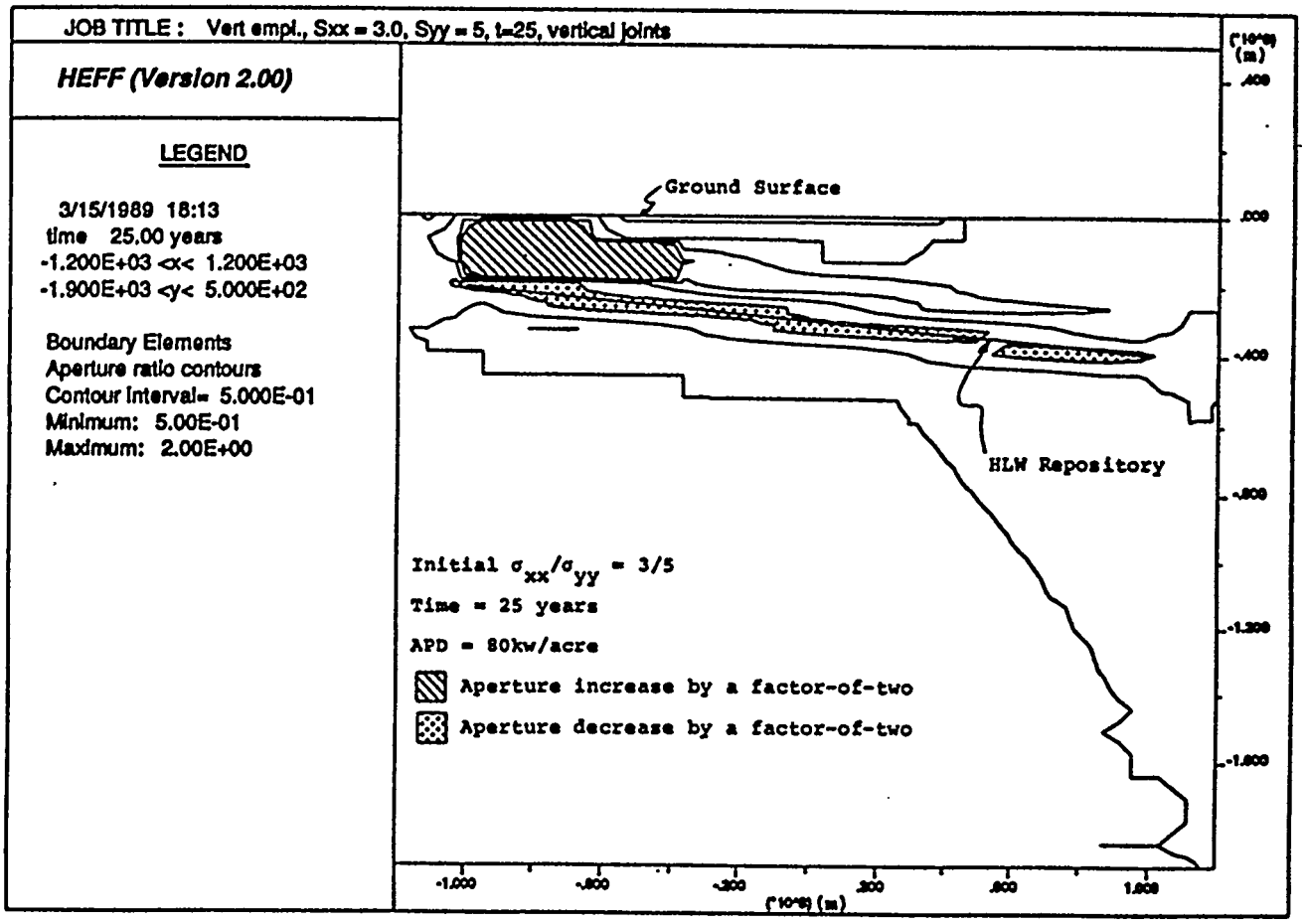

Fig. 37 Regions of Aperture Change by a Factor of Two, 25 Years After Waste Emplacement (σ_{xx}/σ_{yy} = 3/5) [Mack et al., 1989]

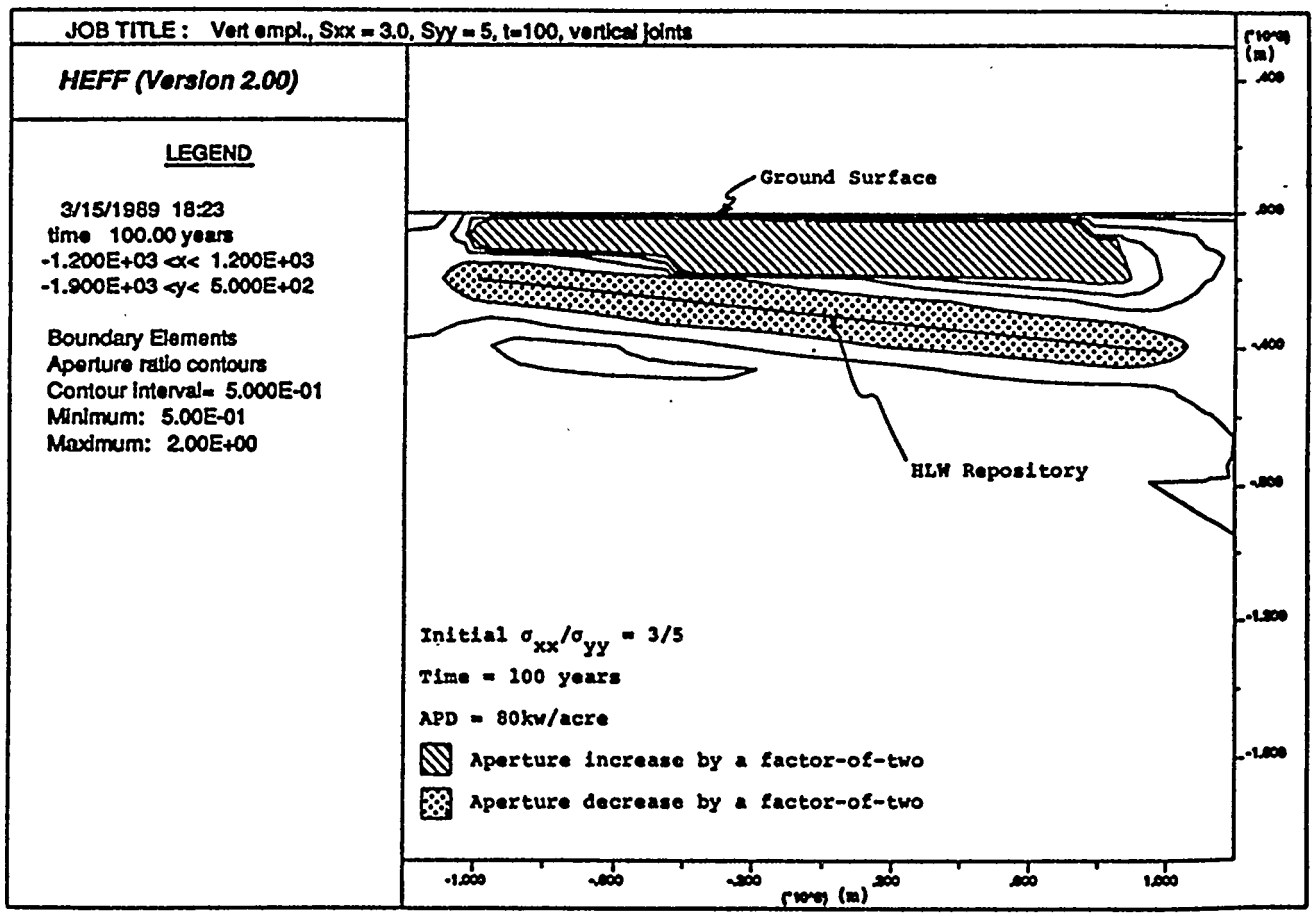

Fig. 38 Regions of Aperture Change by a Factor of Two, 100 Years After Waste Emplacement (σ_{xx}/σ_{yy} = 3/5) [Mack et al., 1989]

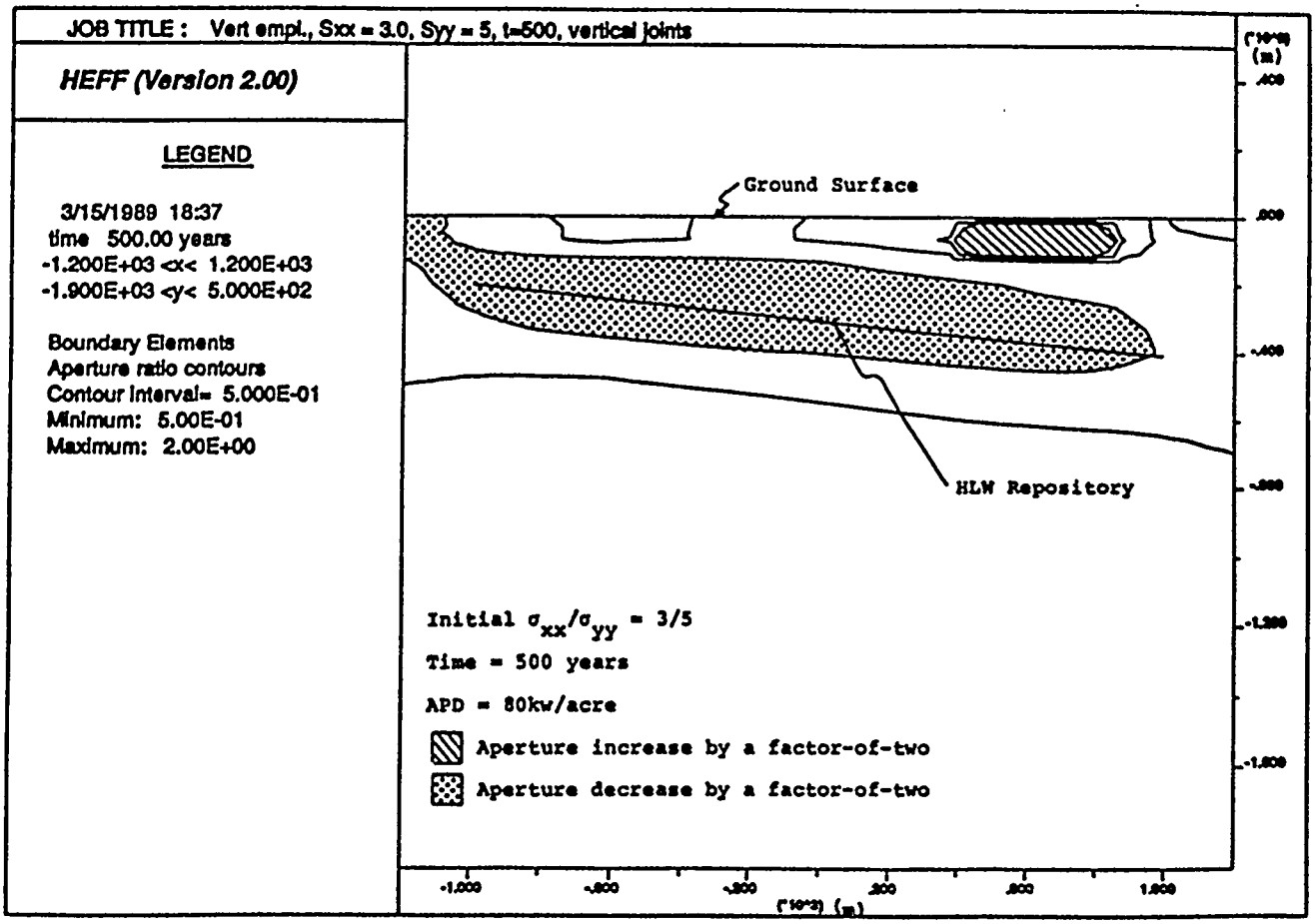

Fig. 39 Regions of Aperture Change by a Factor of Two, 500 Years After Waste Emplacement (σ_{xx}/σ_{yy} = 3/5) [Mack et al., 1989]

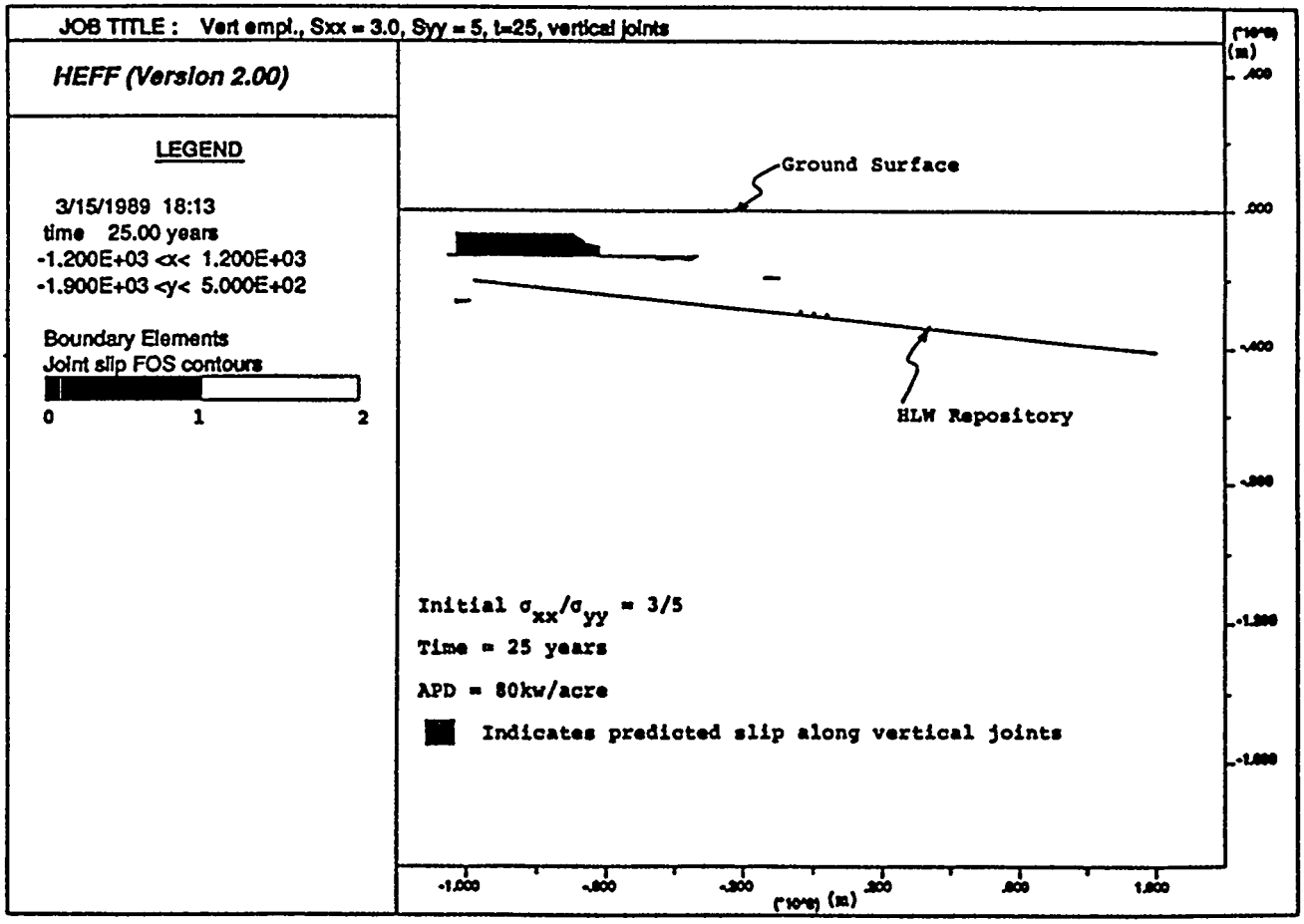

Fig. 40 Region of Predicted Slip Along Vertical Joints 25 Years After Waste Emplacement (σ_{xx}/σ_{yy} = 3/5) [Mack et al., 1989]

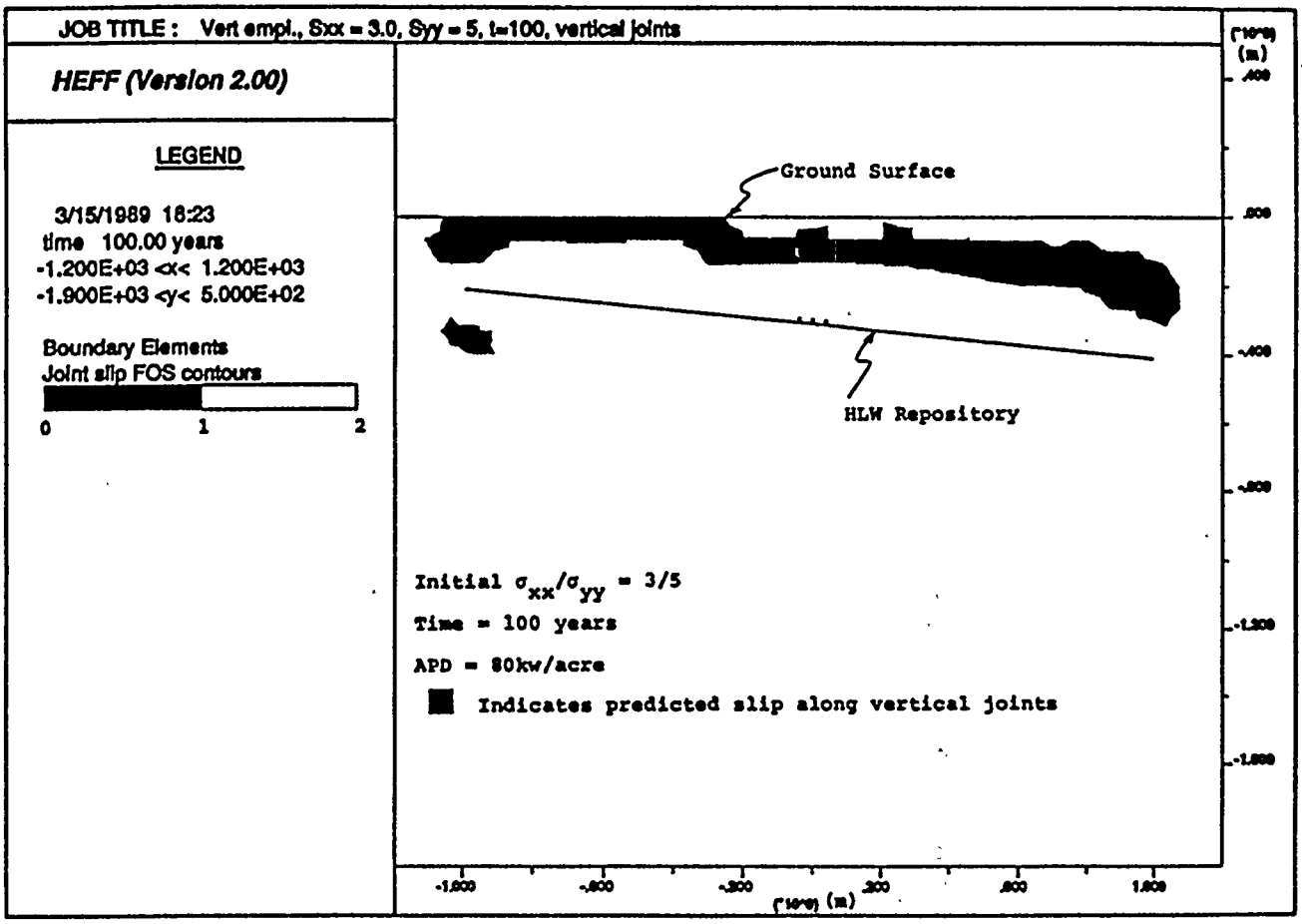

Fig. 41 Region of Predicted Slip Along Vertical Joints 100 Years After Waste Emplacement (σ_{xx}/σ_{yy} = 3/5) [Mack et al., 1989]

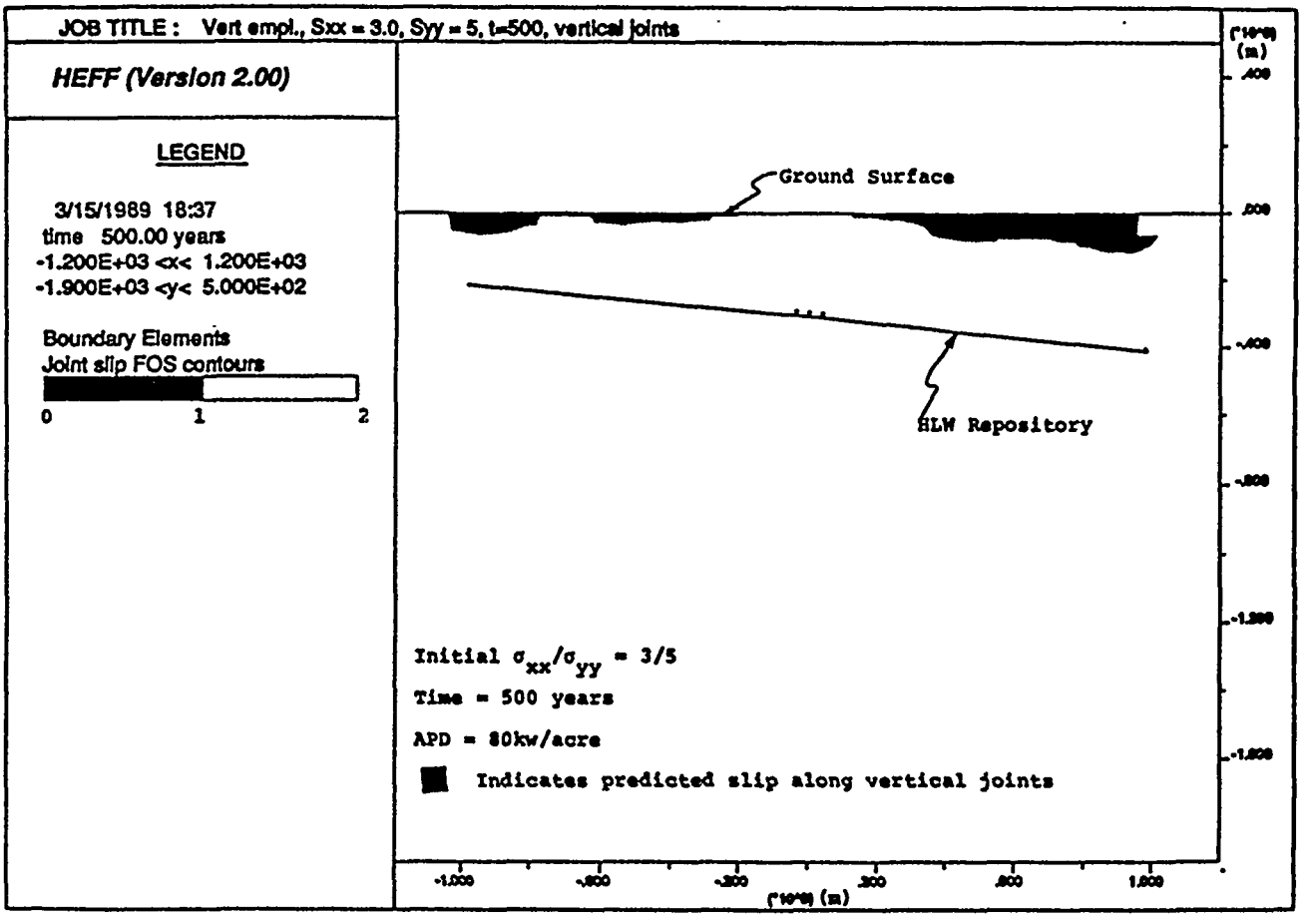

Fig. 42 Region of Predicted Slip Along Vertical Joints 500 Years After Waste Emplacement (σ_{xx}/σ_{yy} = 3/5) [Mack et al., 1989]

The Yucca Mountain site is bounded by fault planes on its northeastern and western boundaries and is cut by the Ghost Dance fault in a rough northwest-southeast direction down its center. Some of these structures indicate significant past displacement. The existence and location of other fault structures within the proposed repository boundaries is unknown and will be explored during site characterization. Several important points need to be addressed regarding the stability of these fault structures: (1) thermally-induced stresses; and (2) dynamic loads from earthquakes and underground nuclear events at the adjacent Nevada Test Site. The maximum slip on these features needs to be determined as a function of time, as well as the radius of slip. Examples of modeling of fault slip behavior can be found in Lemos et al. (1987) and Hart et al. (1988). Models used for examination of fault stability must have the ability to explicitly include the fault in the model. This can be done using a true discontinuum (distinct element) approach, or through the use of interface elements in a continuum code. Whatever approach is used, the fault planes need to allow friction and cohesion along fault surfaces. Because dynamic loading of the faults is of importance, the particular code used needs to allow dynamic wave input to the model.

5.0 CONCLUSIONS

The basic approaches to representation of fractured rock response through modeling were reviewed. In the discontinuum approach, the fractures in the rock mass and the intervening rock blocks are represented explicitly. In the continuum approach, the response of the fractured rock is represented through constitutive models which attempt to account for the important features of the rock response. A continuum approach often is simpler and more efficient to use and, therefore, is desirable if it can adequately represent the true rock behavior. It was discussed that as the ratio of spacing of the jointing with respect to the excavation diameter gets smaller, and as the number of joint sets gets larger, the failure modes should approach those predicted by isotropic plasticity models. However, the behavior of rock masses with limited number of joint sets can be complex, and is determined by the spacing of the joints, the angle of the sets with respect to the principal stresses and the frictional and cohesive properties of the joint surfaces. Depending on these factors, particularly the joint orientation, the behavior can range from an elastic response to one in which wedge failures occur.

In the case of Yucca Mountain, the type of model most suitable for use depends largely on the purpose and geometric scale of the analysis. Site characterization activities thus far have shown that jointing in the Topopah Springs is primarily near vertically oriented with very close spacing. It would appear that this structure will result in some degree of anisotropy in rock response. The degree of anisotropy in the response will be dominated by the properties of the joints and the direction and ratio of the principal stress components. It was shown that, for vertical joints with the assumed range of properties from the SCP, only a limited non-linear response is expected. A ubiquitous or compliant joint representation appears to be adequate for preliminary calculations prior to detailed site characterization in the ESF.

Fault structures which bound and intersect the repository area represent another scale of discontinuity whose response to heating and dynamic loading needs to be examined. A modeling approach in which the faults are represented explicitly is required in this case.

6.0 REFERENCES

Bandis, S. C. "Experimental Studies of Scale Effects on Shear Strength and Deformation of Rock Joints," Ph.D. Thesis, Department of Earth Sciences, University of Leeds, 1980.

Bandis, S. C., A. C. Lumsden and N. K. Barton. "Fundamentals of Rock Joint Deformation," Int. J. Rock Mech. Min. Sci. & Geomech. Abstr., 20(6), 249-268 (1983).

Banerjee, P. K. and R. Butterfield. Boundary Element Methods in Engineering Science. London: McGraw-Hill, 1981.

Barton, N., S. Bandis and K. Bahktar. "Strength, Deformation and Conductivity Coupling of Rock Joints," Int. J. Rock Mech. Min. Sci. & Geomech. Abstr., 22, 11-140 (1985).

Bieniawski, Z. T. "Determining Rock Mass Deformability: Experience from Case Histories," Int. J. Rock. Mech. Min. Sci. & Geomech. Abstr., 15, 237-247 (1978).

Biffle, J. H. "JAC: A Two-Dimensional Finite Element Computer Program for the Non-Linear Quasistatic Response of Solids with the Conjugate Gradient Method," SAND81-0998, April 1984.

Blanford, Mark L., and Samuel W. Key. "An Example of Continuum versus Quasi-Discrete Modeling of a Jointed Rock Mass," in Constitutive Laws for Engineering Materials: Theory and Practice, pp. 1003-1010. Amsterdam: Elsevier Science Publishing, Inc., 1987.

Brady, B.H.G. Heff (Version 2.0), User's Guide. Itasca Consulting Group Report to U.S. Nuclear Regulatory Commission, No. 006-01-40, 1988.

Brady, B.H.G., and E. T. Brown. Rock Mechanics for Underground Mining. London: George Allen & Unwin, 1985.

Brandshaug, T. "Stability of Disposal Rooms During Waste Retrieval," U.S. Nuclear Regulatory Commission, NUREG/CR-5335, March 1989.

Brown, E. T. and J. A. Hudson. "Fatigue Failure Characteristics of Some Models of Jointed Rock," Earthquake Eng. & Struct. Dynamics, 2, 379-386 (1974).

Chen, E. P. A Computational Model for Jointed Media with Orthogonal Sets of Joints. Sandia National Laboratories, SAND86-1122. March 1987.

Christianson, Mark. "Sensitivity of the Stability of a Waste Emplacement Drift to Variation in Assumed Rock Joint Parameters in Welded Tuff," U.S. Nuclear Regulatory Commission, NUREG/CR-5336, April 1989.

Costin, L. S. and E. P. Chen. "An Analysis of the G-Tunnel Heated Block Experiment Using a Compliant-Joint Rock-Mass Model," in Key Questions in Rock Mechanics: Proceedings of the 29th U.S. Symposium (University of Minnesota, June 1988), pp. 625-632. Rotterdam: A. A. Balkema, 1988.

Cundall, P. A. "A Computer Model for Simulating Progressive Large Scale Movements in Blocky Rock Systems," Proceedings of the Symposium of the International Society of Rock Mechanics (Nancy, France, 1971), Vol. 1, Paper No. II-8.

Cundall, P. A. "UDEC - A Generalized Distinct Element Program for Modelling Jointed Rock," Report PCAR-1-80, Peter Cundall Associates; Contract DAJA37-79-C-0548, European Research Office, U.S. Army, March 1980.

Desai, C. S., and J. T. Christian. Numerical Methods in Geotechnical Engineering. New York: McGraw-Hill, 1977.

Fossum, A. F. "Effective Elastic Properties for a Randomly Jointed Rock Mass," Int. J. Rock. Mech. Min. Sci. & Geomech. Abstr., 22(6), 467-470 (1985).

Gerrard, C. M. "Elastic Models of Rock Masses Having One, Two and Three Sets of Joints," Int. J. Rock Mech. Min. Sci. & Geomech. Abstr., 19, 15-23 (1982a).

Gerrard, C. M. "Equivalent Elastic Model of a Rock Mass Consisting of Orthorhombic Layers," Int. J. Rock Mech. Min. Sci. & Geomech. Abstr., 19, 9-14 (1982b).

Goodman, R. E. Introduction to Rock Mechanics. New York: John Wiley & Sons, 1981.

Goodman, R. E. Methods of Geological Engineering in Discontinuous Rock. St. Paul: West Publishing Company, 1976.

Gaziev, E. and Erlikhman, S. "Stresses and Strains in Anisotropic Foundations," in Proceedings of the Symposium on Rock Fracture, ISRM, (Nancy), Paper II-1, 1971.

Hart, R. D., M. Board, B. Brady, B. O'Hearn and G. Allan. "Examination of Fault-Slip Induced Rockbursting at the Strathcona Mine," in Key Questions in Rock Mechanics: Proceedings of the 29th U.S. Symposium (University of Minnesota, June 1988), pp. 369-379. Rotterdam: A. A. Balkema, 1988.

Hocking, G., G.G.W. Mustoe, and J. R. Williams. "Validation of the CICE code for Ice Ride-Up and Ice Ridge Cone Interaction," in Civil Engineering in the Arctic Offshore (Proceedings of the Conference Arctic '85), pp. 962-970. New York: ASCE, 1985.

Hoek, E., and E. T. Brown. Underground Excavations in Rock. London: Institute of Mining and Metallurgy, 1980.

Itasca Consulting Group, Inc. FLAC: Fast Lagrangian Analysis of Continua, User Manual, Version 2.1. Minneapolis: Itasca Consulting Group, Inc., 1988(b).

Itasca Consulting Group, Inc. Universal Distinct Element Code (UDEC), Version ICG1.5 User Manual. Minneapolis, Minnesota: Itasca Consulting Group, Inc., 1989.

Itasca Consulting Group, Inc. 3DEC: 3-D Distinct Element Code, User Manual, Version 1.00. Minneapolis: Itasca Consulting Group, Inc., 1988(a).

Kulhawy, F. H. "Geomechanical Model for Rock Foundation Settlement," J. Geotech. Engr., 104, 211-227 (1978).

Lemos, José. "A Distinct Element Model for Dynamic Analysis of Jointed Rock with Application to Dam Foundations and Fault Motion," Ph.D. Thesis, University of Minnesota, June 1987.

Lemos, J., R. Hart, and L. Lorig. "Dynamic Analysis of Discontinua Using the Distinct Element Method," in Proceedings of the Sixth International Congress on Rock Mechanics (Montreal, 1987), Vol. 2, pp. 1079-1084. Rotterdam: A. A. Balkema and the Canadian Rock Mechanics Association/CIM/CGS, 1987.

MacDougall, Hugh R., Leo W. Scully, and Joe R. Tillerson (Compilers). Site Characterization Plan Conceptual Design Report. Sandia National Laboratoaries, SAND84-2641. September 1987.

Mack, Mark, Terje Brandshaug and Barry Brady. "Rock Mass Modification Around a Nuclear Waste Repository in Welded Tuff," Itasca Consulting Group report to the U.S. NRC, Contract 02-85-002, Topical Report 006-01-T5, July 1989.

Moreland, L. W. "Continuum Model of Regularly Jointed Mediums," J. Geophys. Res., 79, 357-362 (1974).

Singh, B. "Continuum Characterization of Jointed Rock Masses. Part I — The Constitutive Equations," Int. J. Rock Mech. Min. Sci. & Geomech. Abstr., 10, 311-335 (1973).

Stagg, K. G. and Zienkiewicz, O. C. Rock Mechanics in Engineering Practice. New York: John Wiley & Sons, 1968.

Starfield, A. M., and E. Detournay. "Conceptual Models as a Link Between Theory and Practice: A General Approach With a Particular Application to Tunnelling," Rock Mechanics from Research to Application (Proceedings of the 22nd U.S. Rock Mechanics Symposium, MIT, 1981), pp. 398-401. Cambridge, Mass.: MIT, 1981.

Stone, Charles M., Raymond D. Krieg, and Zelma E. Beisinger. SANCHO: A Finite Element Computer Program for Quasistatic, Large Deformation, Inelastic Response of Two-Dimensional Solids. Sandia National Laboratories, SAND84-2618. April 1985.

U.S. Department of Energy (DOE). Consultation Draft Site Characterization Plan, Yucca Mountain Site, Nevada Research and Development Area, Nevada. Nuclear Waste Policy Act, Section 113. January 1988(a).

U.S. Department of Energy (DOE). Site Characterization Plan, Yucca Mountain Site, Nevada Research and Development Area, Nevada, Nuclear Waste Policy Act (Section 113). DOE/RW-0198. December 1988(b).

Zienkiewicz, O. C. The Finite Element Method. London: McGraw-Hill, London, 1977.

Zienkiewicz, O. C., and G. N. Pande. "Time-Dependent Multilaminate Model of Rocks—A Numerical Study of Deformation and Failure of Rock Masses," Int. J. Num. Analy. Methods, 1, 21 (1977)

Zimmerman, Roger M., Robert L. Schuch, Donald S. Mason, Michael L. Wilson, Michael E. Hall, Mark P. Board, Robert P. Bellman, and Mark L. Blanford. Final Report: G-Tunnel Heated Block Experiment. Sandia National Laboratories, SAND84-2620. May 1986(a).

Zimmerman, Roger M., Mark L. Blanford, John F. Holland, Robert L. Schuch, and William H. Barrett. Final Report G-Tunnel Small-Diameter Heater Experiments. Sandia National Laboratories, SAND84-2621. December 1986(b).

NRC FORM 335 (2-89) NRCM 1102, 3201, 3202

U.S. NUCLEAR REGULATORY COMMISSION

BIBLIOGRAPHIC DATA SHEET

(See instructions on the reverse)

1. REPORT NUMBER (Assigned by NRC. Add Vol., Supp., Rev., and Addendum Numbers, if any.)
NUREG/CR-5426

2. TITLE AND SUBTITLE
Examination of the Use of Continuum Versus Discontinuum Models for Design and Performance Assessment for the Yucca Mountain Site

3. DATE REPORT PUBLISHED
MONTH: August YEAR: 1989

4. FIN OR GRANT NUMBER
D1016

5. AUTHOR(S)
M. Board

6. TYPE OF REPORT
Topical Report

7. PERIOD COVERED (Inclusive Dates)
11/88 - 7/89

8. PERFORMING ORGANIZATION – NAME AND ADDRESS (If NRC, provide Division, Office or Region, U.S. Nuclear Regulatory Commission, and mailing address; if contractor, provide name and mailing address.)

Itasca Consulting Group, Inc.
1313 5th Street SE, Suite 210
Minneapolis, MN 55414

9. SPONSORING ORGANIZATION – NAME AND ADDRESS (If NRC, type "Same as above"; if contractor, provide NRC Division, Office or Region, U.S. Nuclear Regulatory Commission, and mailing address.)

Division of High-Level Waste Management
Office of Nuclear Material Safety and Safeguards
U.S. Nuclear Regulatory Commission
Washington, DC 20555

10. SUPPLEMENTARY NOTES

11. ABSTRACT (200 words or less)

This report examines the use of continuum- versus discontinuum-based numerical models for geomechanical design and performance assessment studies at the Yucca Mountain site. Welded tuff is a hard, heavily-fractured rock. The Topopah Springs formation appears, from examination of vertical boreholes, to have a preferred vertical joint orientation. Various constitutive models for representing jointed rock behavior in continuum-based models are reviewed, as well as the discontinuum method. It is concluded that the rock mass is amenable to a continuum plasticity formulation which takes into account the anisotropy introduced by a dominant joint set. Numerous fault structures cross the site. The stability of these structures under thermal seismic loading and their effects on drift stability, seal performance and fluid transport has not yet been investigated. A true discontinuum model allowing dynamic stress analysis is needed in this case.

12. KEY WORDS/DESCRIPTORS (List words or phrases that will assist researchers in locating the report.)

continuum
discontinuum
plasticity
ubiquitous joint
compliant joint
distinct element
fault
joint
Yucca Mountain
Topopah Springs

13. AVAILABILITY STATEMENT

14. SECURITY CLASSIFICATION
(This Page)
(This Report)

15. NUMBER OF PAGES

16. PRICE

*U.S. GOVERNMENT PRINTING OFFICE:1989-241-590:00218